Chapter 18
Oleogel Characterization: Physical, Physicochemical, and Chemical Techniques

Fernanda Peyronel and Elena Dibildox-Alvarado

Abbreviations

AED	Atomic emission detector
AFM	Atomic force spectroscopy
AOCS	American Oil Chemists Society
APCI	Atmospheric chemical ionization
BFM	Bright field microscope
C	Circularity of aggregates
CAN	Crystalline aggregates number
Cryo	Cryogenic
DAPI	4′,6-Diamidino-2-phenylindole
DLS	Dynamic light scattering
DSC	Differential scanning calorimeter
ECD	Electron capture detector
ED	Equivalent diameter of aggregates
ELSD	Evaporative light scattering detection
EM	Electron microscopy
FA	Fatty acid
FID	Free Induction Decay
FTIC	Fluorescein-5-isothiocyanate
FW	Fruit waxes GC gas chromatography

F. Peyronel (✉)
Food Science Department, University of Guelph, Guelph, ON, Canada
e-mail: fsvaikau@uoguelph.ca

E. Dibildox-Alvarado
Facultad de Ciencias Químicas, Laboratorio de Biopolímeros Alimentarios, Universidad Autónoma de San Luis Potosí, San Luis Potosi, Mexico
e-mail: dibildox@uaslp.mx

C. Andrea Palla, F. Valoppi (eds.), *Advances in Oleogel Development, Characterization, and Nutritional Aspects*,
https://doi.org/10.1007/978-3-031-46831-5_18

GLC	Gas-liquid chromatography
GSC	Gas-solid chromatography
HF	Heat-Flux
HPLC	High-Pressure Liquid Chromatography
L	Length of aggregates
LEC	Soya lecithin
MDGC	Multidimensional gas chromatography
MPL	Metal-phosphate luminophores
MRS	Magnetic resonance spectroscopy
NMR	Nuclear magnetic resonance spectroscopy
OM	Weight of solid
OOO	Triolein
OSI	Oxidative stability index
PC	Power-compensated
PLM	Polarized light microscopy
pNMR	Pulsed nuclear magnetic resonance
PP	Penalty point
PV	Peroxide value
PV-LED	Peroxide value light emitting diode
SEM	Scanning electron microscopy
SFA	Saturated fatty acid
SFC	Solid fat content
SSS	Tristearin
SW	Weight of oil
TAGs	Triacylglyceride
TCD	Thermal conductivity detector
TEM	Transmission electron microscopy
Tg	Transition temperature
TPA	Texture profile analyzer
TW	Weight of oleogel
UV/VIS	Ultraviolet/visible

18.1 Introduction

Various approaches can be employed to structure oleogels, with the help of molecules called oleogelators. The structures that the oleogelators can form are confined within oily matrices that are typically free of *trans* fats and low in saturated fatty acids. Oleogels can be produced by utilizing one or multiple oleogelators within a singular oil or a blend of oils and can also be structured using water to form different types of emulsions, such as simple or bigels (w/o, o/w).

In order to design effective strategies for studying and evaluating these structures, as well as the behavior and stability of oleogels during shelf life, it is crucial to select

Table 18.1 Techniques and methods to be discussed in this chapter that can be used to study oleogels

Structure analysis (mm, μm, nm, atomic scale)		Chemical characterization	Thermal characterization
18.2.1 Cone penetration test	18.2.6 DLS	18.3.1 Raman	18.4.1 DSC
18.2.2 Compressed test	18.2.7 Cryo SEM and Cryo TEM	18.3.2 FTIR	
18.2.3 Oil migration test	18.2.8 Confocal microscopy	18.3.3 GC	
18.2.4 Oil flowing test	18.2.9 AFM	18.3.4 HPLC	
18.2.5 PLM/BF microscopy	18.2.10 Pulsed NMR	18.3.5 Oxidative stability	

appropriate methodologies. Predictions based only on the oleogelator and oil to use are frequently insufficient in achieving an accurate diagnosis. Therefore, it is important to choose or adapt analytical techniques based on the desired final structure and matrix of the oleogel, as well as the parameters to be evaluated.

This chapter describes the basics of many analytical techniques and some methods that can be applied to the characterization of oleogels and is focused on the results obtained from them, highlighting their use and how they have been implemented in the study of oleogels. Each technique or method brings a different insight into the oleogel structure; hence, the choice of which one to use depends on the final objective. Usually, the desired application of the oleogel dictates the parameters needed to be evaluated; hence, different techniques might be required. Table 18.1 lists the techniques that will be discussed in this chapter.

Additionally, this chapter will provide a detailed examination of the penalty points (PPs) associated with each technique, along with strategies to minimize these points using the Eco-Scale—an analytical methodology devised by Gałuszka and colleagues [1, 2]. The Eco-Scale employs the principles of "Green Chemistry" [3, 4] to rate a process in terms of its environmental and human health impact. PPs are utilized by the Eco-Scale to quantify the harm caused by reagents, solvents, and equipment based on their environmental and health impact. Methods with higher PPs are deemed to be more hazardous. Therefore, the aim is to select reagents, solvents, and equipment that result in the least amount of PPs.

To mitigate the PPs resulting from reagents and solvents, several strategies can be adopted, including the elimination or substitution of toxic compounds, or the reduction in their quantity. The energy consumption of equipment can also be curbed by utilizing devices that are more efficient or limiting their operation duration. Furthermore, the principles espouse the adoption of multi-analyte or multi-parameter methods, sample number and size reduction, and avoidance of derivatization. These guidelines not only serve to decrease the impact of the analytical process on the environment and human health but also ensure the safety of operators. The Eco-Scale also takes into account the PPs associated with waste disposal during the analytical process. However, the focus of this chapter is on the PPs resulting from by

the use of reagents, solvents, and energy consumption by the equipment. The quantification of the PPs of each chemical (reagent or solvent) [1, 2] will be calculated as follows:

$$\text{PPs} = \text{PP reagent/solvent amount} \times [\text{Pictograms PP} + \text{Hazardous PP}] \quad (18.1)$$

PP reagent/solvent amount is a number (0, 1, 2, 3) based on the amount of reagent/solvent used as described in the Eco-Scale. Pictogram PP refers to 0, 1, 2, etc., according to the number of WHMIS-regulated pictograms associated with the reagent or solvent. Hazardous PP refers to 0, 1, or 2 depending if the label of the chemical has no warning word (0), or if the word "warning" (1) or "hazard" (2) is displayed on the label. The amount of energy consumed by the equipment will also be estimated based on the penalty points assigned by the Eco-Scale [1, 2]. The total PPs will be determined by adding the PPs associated with all the chemicals used, including the PPs attributed to the energy consumption resulting from the operation of the equipment.

Each section expands on the principles of the technique or method, including recommendations on its application to oleogels, and presents data obtained via selected technique or method. In order to provide a concise summary of each technique or method, a four-column table has been constructed and placed at the end of each section. The four-column table details the spatial length scale that the technique can investigate, the equipment operating cost (condensed as "$" for low, "$ $" for medium, and "$$$" for high), the parameters that can be measured using the technique, and the corresponding PPs.

18.2 Structure Analysis Techniques

18.2.1 Cone Penetration Test

The cone penetration test is a widely used technique to evaluate the consistency or hardness of soft materials such as butter or animal/vegetable spreads and semisolid fats [5–7]. Traditionally, a metal cone is dropped into the material, and an analog dial reports the results. While the manual cone penetrometer instrument is still used by many research groups, digital versions are now being manufactured.

A cone penetrometer consists of a stand to which a metal shaft is attached, with either a dial or a digital screen connected to the shaft. Different probes can be attached to the end of the shaft, with the cone being the most popular. The choice of probe depends on the anticipated range of firmness of the material to be analyzed. Harder samples require probes with a smaller diameter or a smaller cone angle. The probe is positioned directly above the surface of the sample with penetration occurring under the probe's dead weight. Attention is needed to ensure that the specimen's surface is smooth and flat.

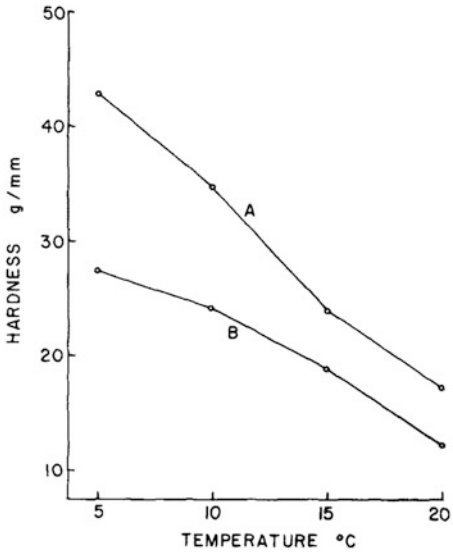

Fig. 18.1 Changes in hardness with increase of the temperature for butter (A) and margarine (B). (Reproduced from [5] with permission from AOCS Press)

There are two modes of operation: one involves releasing the cone for a certain length of time, while the other involves letting go of the cone and waiting until it comes to a stop. This allows for a rapid empirical evaluation of the material's properties. Oleogels, which fall into this category of soft materials, can also be analyzed using a cone penetrometer.

The results of cone penetration are typically interpreted in terms of the depth of penetration, regardless of the method used to stop the movement of the cone. In order to maintain consistent conditions, various recipes are tested with constant cone angle, mass of the dropping assembly, and temperature. de Man [5, 8] demonstrated a correlation between penetration depth and hardness in butter, due to thixotropic changes, when the cone was allowed to move for 5 s. For example, Fig. 18.1 illustrates the changes in hardness with temperature for butter and margarine, where penetrometer depths were converted to hardness using the equation: hardness = (mass of the cone assembly)/(depth of penetration in mm obtained from [5]).

The analysis of the yield value of a material is influenced when employing the approach where the probe is allowed to come to rest. During this process, the applied stress decreases until it reaches the yield value, at which point the material's deformation ceases. In 1959, Haighton [6] demonstrated that the logarithm of the penetration is inversely proportional to the logarithm of the yield value, and proposed a relationship between yield and depth of penetration for fats and margarines. However, it should be noted that some oleogels might be too soft to be probed with a heavy cone. Furthermore, as this instrument does not provide absolute results, selecting an alternative cone for comparison is not a concern unless a standardized method, such as method Cc 16–60 from AOCS [9], is being followed [9].

Penalties Points

The absence of solvents to run the equipment means that there are no PP created by chemical use. Additionally, the manual version of the cone penetrometer does not generate PP from electricity, while the digital version is used for such a brief time, that there is no PP created due to electricity. Therefore, the technique's overall PP value is zero.

Relevant Information Regarding the Technique

Spatial length scale	Operation of equipment ($, $$, $$$)	Parameters to measure	Penalty points
Millimeters	$	Spreadability Firmness	0

18.2.2 Compressed Test

A texture profile analyzer (TPA) is a widely used instrument for conducting compression tests on food materials. Various designs are available in the market, featuring either one or two vertical arms with a horizontal section to which the probe is attached. The probe is lowered and raised with great precision using a control system. During a TPA test, the sample is placed on the platform beneath the probe, and the horizontal arm with the attached probe is lowered to penetrate the sample. The test measures the strain, stress, and force required to compress, break, or penetrate the sample, which are registered during the test. One type of measurement is to control the rate of probe penetration until a specific final depth is reached (back extrusion or strength test) while recording the force exerted by the probe [10, 11]. Another type of measurement involves performing two consecutive compression cycles to simulate "mastication." This test generates rapid results and provides information on the sample's main textural parameters, such as firmness, adhesiveness, springiness, cohesiveness, elasticity, gumminess, and chewability. Regardless of the method used, force is the key parameter, and force versus time or distance (as deformation or displacement) is typically recorded.

A typical TPA double compression test measurement is illustrated in Fig. 18.2, where the Szczesniak mastication profile was used to identify parameters. The most commonly used variables in such tests include hardness, the maximum force required to compress the sample which is the height of the first peak; adhesiveness, which is the first negative area; cohesiveness, or the extent to which the sample could be deformed prior to rupture which is the second positive area divided by the first positive area; springiness, or the ability of the sample to recover its original form after deformation is removed, which is the time of second bite divided by the time of first bite; gumminess, or the force needed to disintegrate a semisolid sample to a steady state of swallowing which is hardness multiplied by cohesiveness; chewiness,

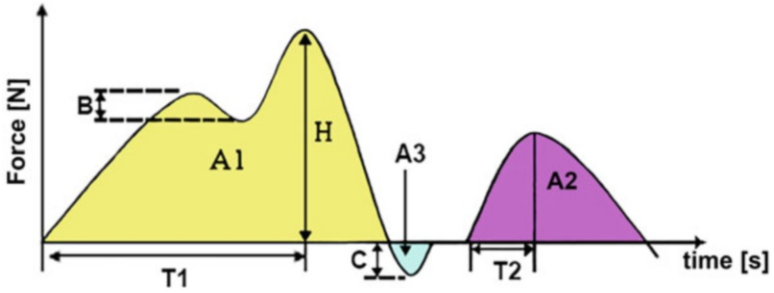

Fig. 18.2 Texture analyzer profile using Szczesniak profile. B = brittleness, H = hardness, C = cohesion strength, T1 = indentation, A3 = adhesiveness, A2/A1 = cohesiveness, T2/T1 = elastic quality, H × A2/A1 × T2/T1 = masticability, H × A2/A1 = gumminess. (Reproduced from [12] with permission from Elsevier)

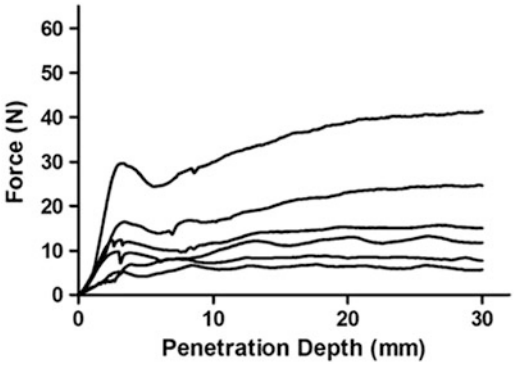

Fig. 18.3 Back extrusion results on an oleogel made using canola oil and 15% ethyl cellulose. (Reproduced from [10] with permission from Elsevier)

or the work needed to chew a solid sample to a steady state of swallowing which is gumminess multiplied by springiness. Brittleness refers to the fracture behavior where the more force indicates less brittle; indentation is the force needed to keep a permanent deformation.

Each area in Fig. 18.2 provides a number that can be compared between samples. However, the lack of "standards" makes it difficult to carry out quantitative measurements with this instrument. Nevertheless, using a TPA removes the subjectivity of panelists and allows for sample comparisons, although it is important to conduct comparisons under the same experimental conditions. This technology is particularly useful when comparing oleogels made with different amounts or types of oleogelators. A control product that consumers accept as optimal can be used "as a standard".

When the samples are too soft, the mastication profile may not be adequate, and in such cases, the TPA can be used for extrusion. This is applicable for oleogels, as shown in Fig. 18.3, which displays the result of a back extrusion measurement using a probe that was moved at 1.5 mm/s for an oleogel made with 15 wt% ethyl cellulose in canola oil, as reported by Gravelle and colleagues [13].

Table 18.2 Results of a TPA test on oleogels made using various olegelators in rapeseed oil

Oleogelator	Maximum force of deformation (N)	Hardness (N)	Work of shear (N. mm)	Stickiness (N)
CAN (2%)	5.52 ± 0.33	12.68 ± 1.06	35.57 ± 3.88	−10.06 ± 0.83
MAG (5%)	0.77 ± 0.15	6.47 ± 0.46	18.29 ± 1.34	−7.50 ± 0.31
BW (3%)	1.60 ± 0.31	5.60 ± 0.42	13.00 ± 1.05	−6.22 ± 0.39
BY (3%)	0.73 ± 0.15	4.39 ± 0.42	9.74 ± 1.44	−4.87 ± 0.41
SUN (1%)	3.33 ± 0.42	15.78 ± 3.12	46.62 ± 8.60	−20.37 ± 4.53

Adapted from [11]
Work of shear was determined as the area given by A1 in Fig. 18.2. Stickiness was determined as the cohesion strength (C) in Fig. 18.2

Kupiec and colleagues [11] compared different oleogels made with various olegelators in rapeseed oil. Those authors used different oleogelators, such as candelilla wax (CAN 2%), monoglycerides (MAG 5%), yellow beeswax (BW 3%), white beeswax (BY 3%), and sunflower beeswax (SUN 1%), with each number in the brackets representing the weight percentage. Table 18.2 summarizes the results obtained by the group. For statistics, please refer to the original paper.

By looking at the results on Table 18.2, conclusions about different characteristics of the oleogels can be easily made.

Penalty Points

This test does not require any reagents or solvents, resulting in a PP of 0 for chemical usage. In addition, the electricity consumption is minimal, using less than 0.1 kWh, resulting in a PP of 0 for electricity usage.

Relevant Information Regarding the Technique

Spatial length scale	Operation of equipment ($, $$, $$$)	Parameters to measure	Penalty points
Millimeters	$	Firmness Adhesiveness Springiness Cohesiveness Elasticity Gumminess Chewability Spreadability	1

18.2.3 Oil Migration Test

Oil migration is a diffusion-based movement [14] of liquid oil from an oil-rich phase to a lipid-poor or lipid-solid phase in a food product. This phenomenon is observed in various products, including cream-filled cookies, chocolate-coated goods, multilayer filled chocolate products, and many composite products that are coated with chocolate. The oil migration can result in various quality issues, including changes in

texture and flavor, reduced shelf life, and decreased product appeal. Factors that affect oil migration include the composition and structure of fats and oils, processing techniques, and temperature and storage conditions. Fats with high melting points and high solid content tend to have lower oil migration rates. Products containing emulsifiers can enhance structural stability and prevent oil migration. Failure to control oil migration can lead to quality issues such as fat bloom, softening of chocolate, and hardening of the filling. The phenomenon of oil migration is closely related to the structural properties of the lipid's crystal lattice, which determines its oil-retaining ability [15].

Various techniques can be utilized to investigate oil migration, including fluorescence recovery after photobleaching [16], magnetic resonance imaging [17], compression test, differential scanning calorimetry (DSC), X-ray diffraction, and many different microscopy techniques. All those techniques require specialized equipment. However, there are two methods commonly employed that do not necessitate sophisticated instrumentation. They are the time-dependent monitoring of stained oil using a dye, such as Nile red [18], and the gravimetric method [15].

The stained-oil method involves adding Nile red to the material, which binds to the lipids and allows for visual observation of the stained oil. The measurement is performed using a flatbed scanner, with the pixel intensity used to determine the amount of migrated oil [18]. In contrast, the gravimetric method involves forming the processed sample into discs, which are stored at specific temperatures for a specified period before analysis. Multilayered discs can also be utilized to facilitate or enhance analysis. The disc is placed on top of a filter paper to allow the oil to flow toward the paper using only gravity as the driving force. The method enables the determination of oil loss from the fat crystal network by weighing the filter papers (wt. paper) and the sample disc (wt. disc) before (t=0) and after storage (t) [15]. Oil loss is calculated using the following formula:

$$\text{Oil loss} = \frac{\text{wt.paper } (t) - \text{wt.paper } (t=0)}{\text{wt.disc } (t=0)} \times 100\%$$

However, there are no official standards set in the food industry for either of these two methods. For instance, the amount of Nile red added is arbitrary, and the size and weight of the sample discs are also arbitrary. Thus, each research group can choose which absorbent paper to use, the number of hours or days the sample rests on the paper, and the storage temperature. It should be emphasized that these two inexpensive and straightforward methods are useful for sample comparison only. For example, Cho and colleagues [19] recently employed the gravimetric method to quantify oil and water losses in frozen/thaw edible rice bran wax-gelatin biphasic gels. The authors found that after one freeze-thaw cycle, the biphasic gels had less total liquid loss by approximately 50% compared to the oleogels.

Penalty Points

When considering the gravimetric method, there are no penalty points since no reagents or solvents are involved, and no equipment that consumes electricity is required. In the case of time-dependent monitoring of stained oil using a dye, Nile

red carries with it 0 penalty points when the amount is less than 10 mL or 1 PP when it is between 10 and 100 mL. The energy consumption for the scanner can be between 1 and 2, depending on penalties points (when energy is below 1.5 kWh) and up to 2 PPs. Hence, the maximum for this method could be 2 PPs.

Relevant Information Regarding the Method

Spatial length scale	Operation of equipment ($, $$, $$$)	Parameters to measure	Penalty points
Nanometers to micrometers	$	Weight of oil displaced Color intensity	0–2

18.2.4 Oleogel/Oil Flowing Test

The flowing test is a simple method used to determine the minimum concentration of an oleogelator required to produce a material that does not flow under its weight. The material to be studied is placed inside a vial and either inverted or centrifuged after a certain time. If the material does not flow after inversion or if there is no separation when using the centrifuge, then the material can be called an oleogel.

When using the direct method to make oleogels, the oleogelator is dissolved in the oil phase at sufficiently high temperatures to generate a solution, and then stirred for some minutes before it gets cool down, usually to ambient conditions. The time needed for the oleogel to set can range from hours to weeks. Once the desired period has elapsed, vials containing the samples are turned upside down or inserted in a centrifuge. The critical concentration is determined by visually comparing the vials. The vial that uses the lowest amount of oleogelator and does not flow or separate is identified as the one with the "critical concentration." Vials are typically prepared using increments of 1% of the oleogelator. Critical concentrations for specific oleogelators in specific oils can be found in the literature. However, changing the oil or oleogelators may require repeating the flowing test.

Centrifugation can be used to determine the weight of the non-gelated oil. The method employed during centrifugation is referred to as the "oil binding capacity," which determines the quantity of oil released from the sample following the centrifugal process. To measure how much oil is liberated, the weight of the oleogel placed in the tube for centrifugation is measured (TW). After centrifugation, the tube is inverted, and the non-bound oil is collected and weighed (OW). The weight of the solid remaining in the tube can be calculated as $SW = TW - OM$. Sometimes, the percentage of oil liberated (or not trapped in the solid matric) is calculated using the formula $(SW - OW)/(TW - SW) \times 100$. This allows for a quick comparison between samples. However, there are no standards for the weight of the oleogel or the parameters to use during centrifugation. Each research group must exercise their discretion in determining the weight of the sample to centrifugate and the parameters to use in the centrifuge (e.g., speed of rotation or temperature).

Penalty Points

There are no penalty points associated with the oleogel/oil flowing test (or inversion method), as there are no reagents or solvents involved and no consumption of electricity. When the centrifuge is used, the energy required to run the centrifuge (electricity ≤1.5 kWh) can generate 1 penalty point.

Relevant Information Regarding the Method

Spatial length scale	Operation of equipment ($, $$, $$$)	Parameters to measure	Penalty points
Millimeters	$	Visual flow of material	0–1

18.2.5 Polarized Light and Bright Field Microscopy (PLM/BFM)

18.2.5.1 Polarized Light Microscopy

Polarized light microscopy (PLM) is a robust contrast-enhancing technique that exploits the unique optical properties of anisotropy to reveal valuable information on the structural and compositional properties of diverse materials, such as oleogelators in oleogels. A PLM is a bright field microscope in which the sample is illuminated with oriented single plane waves, by positioning a polarizer between the light source and the specimen, and an analyzer between the objective rear aperture and the observation tubes or camera port. This technique utilizes the optical properties of anisotropy to reveal information about the structure and composition of materials [20], enabling the differentiation of isotropic and anisotropic materials. PLM has proven to be a useful technique to identify solid crystals in edible fats [21, 22] because solid fat crystals are birefringent, hence appear bright under polarized light. PLM can be used for both qualitative and quantitative analysis to provide insights into the morphology and organization of the oleogelator in the sample.

The solid structure of an oleogel can be determined by placing approximately 10 μL (a drop) of the sample onto a microscope slide and covering it with a cover slide (Fig. 18.4). It is important not to add too much sample as it must be squeezed with the cover slide. Alternatively, some oleogels that are manufactured using the direct method can be formed directly on the microscope stage. In this case, the oil and oleogelator are pre-mixed and a drop of the mixture at room temperature is deposited on the microscope sample holder. The pre-mixed sample is then subjected to a temperature cycle, which may include thermal memory elimination, continuous or intermittent cooling ramps, or isothermal structuring periods. Sometimes, a shear cycle may also be applied. These techniques can be performed using a microscope that has the necessary capabilities (e.g., cold stage using liquid nitrogen (Fig. 18.4)

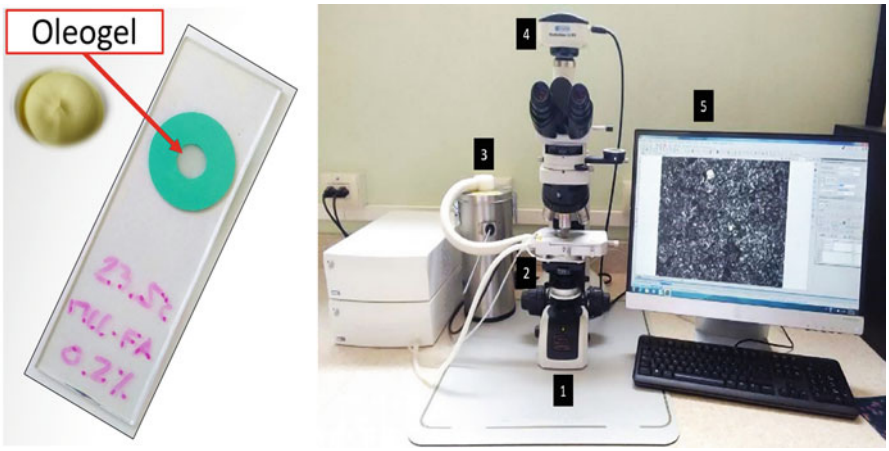

Fig. 18.4 Location of an oleogel in the microscope slide and the equipment used to capture PLM images: (1) Body of the microscope. (2) Temperature control stage. (3) Liquid nitrogen reservoir. (4) Camera. (5) Image analysis software for managing the information collected during the measurement. (*Source*: Courtesy of Food Biopolymer Lab, Faculty of Chemical Sciences of the Autonomous University of San Luis Potosí)

or shear cell). A note to make here is that one needs to be aware that the material is "not free" to expand in three dimensions, but it is rather confined to the small space between the microscope slide and its cover slip.

Most microscopes are equipped with objectives of different magnifications, ranging from low (~4 or 5X) to the highest of all, usually 100X. The selection of the objective depends on the size of the structures to be observed. Images can be recorded as a function of the structuring oleogelator and/or storage time of the oleogel, or as a function of the temperature. The shapes and sizes of the structures formed can be evaluated by image analysis. An optical microscope is limited in the resolution and the smallest particles that can be measured, usually limited to micrometer sizes. Free software for image analysis is accessible on the web, or commercial software can be used for more measurements that are specialized. To perform these measurements, it is necessary to convert the acquired grayscale images to binary images [23] (as shown in Fig. 18.5 for the case when the temperature was 23.5 °C). It is advisable to take measurements from at least four different micrographs of the oleogel sample. The data is typically reported as the mean and its standard deviation.

A grayscale image is normally obtained by capturing the light reflected from the sample onto the sensor of the camera. To obtain a binary image, a threshold must be applied to the grayscale image. The threshold is a value chosen to separate the foreground (the structures of interest) from the background (the rest of the image). The threshold is needed to identify where the particle of interest has its outer limit. Pixels with a value above the threshold are set to white and those below the threshold are set to black. This process creates a binary image where the structures of

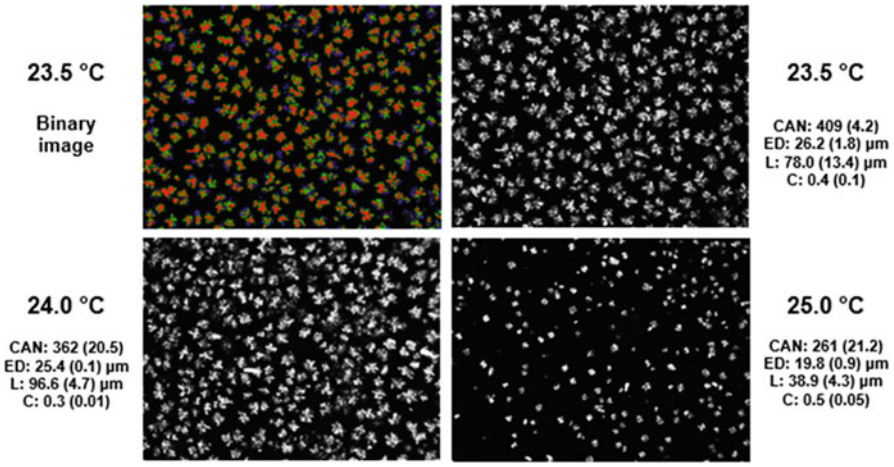

Fig. 18.5 PLM microphotographs showing the water-in-palm oil emulsions crystallized at three different isothermal temperatures using microcrystalline cellulose as the oleogelator. (CAN: Crystalline aggregates number. ED: Equivalent diameter of aggregates. L: Length of aggregates. C: Circularity of aggregates). (*Source*: Courtesy of Food Biopolymer Lab, Faculty of Chemical Sciences of the Autonomous University of San Luis Potosí)

interest are highlighted in white, and the background is in black. This binary image can then be used for image analysis to obtain parameters such as crystal number, area, equivalent diameter, perimeter, length, width, circularity, elongation, intensity, among others. A binary image can easily be colored with the right software. Figure 18.5 displays four parameters of a water-in-palm oil emulsion using microcrystalline cellulose as structuring agent and prepared at three different temperatures. These parameters can aid in the interpretation of the observed changes in crystalline structure over time.

18.2.5.2 Bright Field Microscopy

A bright field microscope (BFM), also referred to as a compound light microscope, is an optical microscope that uses light rays to produce a dark image against a bright background [24]. While some BFM are designed exclusively for bright field mode, this instrument can be used as a polarizing light microscope (PLM) by adding a polarizer and an analyzer in the light path. Both qualitative and quantitative analyses can be performed using a BFM, similar to the PLM. Qualitative analysis is relatively straightforward when there are noticeable differences in the morphology, size, and number of structures present in the images. However, quantitative analysis requires a mathematical approach that involves measuring specific features. The selection of relevant features is a crucial step, which necessitates some expertise on the operator. Nowadays, software packages that accompany microscopes, or freely accessible

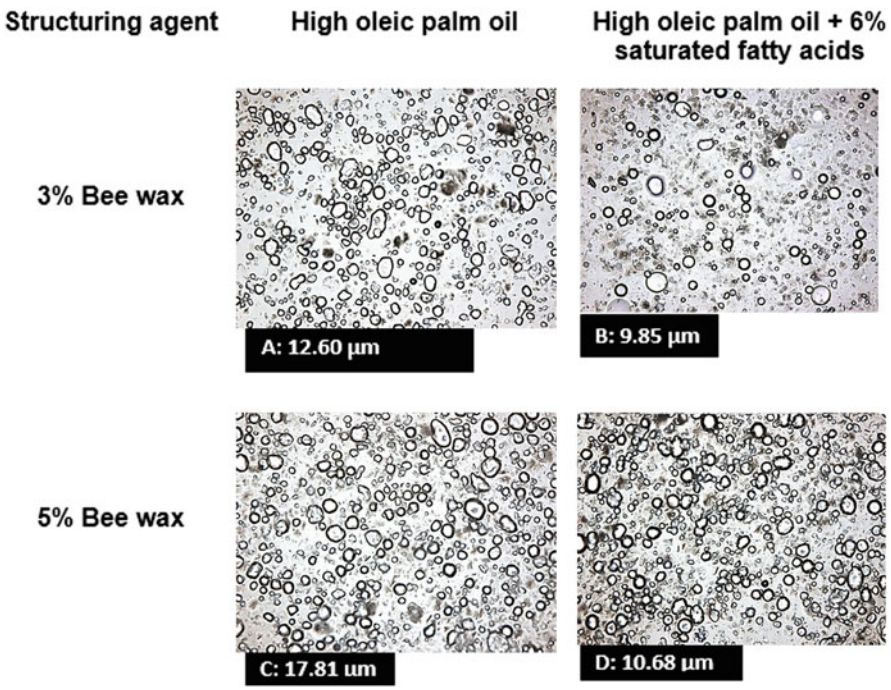

Fig. 18.6 Microphotographs taken in bright field mode using a 20× objective of oleogelled emulsions containing 3% (**a**, **b**) and 5% (**c**, **d**) beeswax, and high oleic palm oil with different content of saturated fatty acids: 32% (**a**, **c**), 38% (**b**, **d**). The number indicates the average equivalent diameter of the water droplets. (*Source*: Courtesy of Food Biopolymer Lab, Faculty of Chemical Sciences of the Autonomous University of San Luis Potosí)

ones, can be used for quantification. Quantitative analysis enables accurate comparison of samples, and in the case of gelled and bigellated emulsions, bright field microscopy provides a straightforward way to calculate droplet size and distribution in the emulsion.

Figure 18.6 demonstrates the influence of varying concentrations of beeswax gelling agent (3% and 5% of beeswax) and the quantity of saturated fatty acid (SFA) present in high oleic palm oil (32% and 38% SFA) on the water drop size of a gelled water-in-oil emulsion. The impact of differing concentrations of gelling agent and solids in the oleogel is visually apparent from the increased number of water droplets of varying sizes. However, a more comprehensive analysis of the effect can be achieved by determining the equivalent diameter using image analysis techniques, or better still, obtaining a histogram or curves that provide a clear representation of the droplet size distribution present in the emulsion.

Penalties Points

The energy consumption of both BFM and PLM instruments is less than 1.5 kWh, resulting in a PP = 1. However, if the analysis of the oleogel requires temperatures below ambient, liquid nitrogen is necessary, and the cost of the nitrogen must be considered. As liquid nitrogen is classified as a hazardous material with a warning symbol, it carries a PP of 2 × (1 + 1) = 4.

Relevant Information Regarding the Technique

Spatial length scale	Operation of equipment ($, $$, $$$)	Parameters to measure	Penalty points
Micrometers to millimeters	$$$	Crystal sizes Crystal number Crystal morphologies and dimensions	1–4

18.2.6 Dynamic Light Scattering

Dynamic light scattering (DLS) is a non-invasive technique commonly used to characterize particles, whether they are in a solution or as powders. Dynamic means that there is movement, which can be created by Brownian motion or because the instrument moves the particles to be measured. Light scattering refers to the use of "light", usually a laser and the phenomena of scattering. We are here discussing an instrument that "moves" the particles to be analyzed, like a Mastersizer. This method does not require calibration standards, but it does necessitate the measurement of an empty sample holder before the sample measurement, similar to other scattering techniques. The empty sample holder is automatically measured by the instrument prior to collecting data for the sample, and the software automatically removes the background from the sample before showing the results. However, the user can prevent this from happening by consulting the relevant manuals.

In principle, this measurement technique involves unperturbed laser light shining on particles, which scatter the light. The instrument's detectors register the intensities as a function of the scattered angle. At the molecular level, this can be understood as incoming photons interacting with the electron density of the atoms in the sample. The interaction between photons and electrons results in the emission of photons at various angles, which the detectors capture. The scattering theory employs the scattering q-vector as the variable, and the raw data collected by the instruments represent the magnitude of the scattering q-vector versus intensity, which is the number of photons counted at each detector.

The software utilized for data analysis employs the widely accepted Mie theory, which reports data as a function of either volume density or surface density of particles with respect to particle size, rather than intensity with respect to the magnitude of the q-vector. Alternatively, the Fraunhofer approximation can be used in lieu of the Mie theory. The Mie theory uses a spherical or non-spherical particle, chosen by the user, to model the collected data. Therefore, when the data is displayed on the screen, it is reported as the volume density on the *Y*-axis versus the particle size on the *X*-axis. Have in mind, that this data have already been processed, and is not the raw data. The idea of the manufacturer is to simplify the user's work by showing results of the correct model that fits the data best. The "model" requires particle and media related parameters such as refractive index, absorption indexes for the equipment's two lasers, and densities. The user also selects if the particles are spherical, non-spherical or opaque in order for the model to accurately compute the surface distribution or the volume distribution.

In a liquid measurement, the sample is dispersed in a medium (dispersant) and kept in constant motion to prevent flocculation while simultaneously diluting the sample. Dilution is crucial to prevent multiple scattering, which arises when many particles are present. Prior to analysis, the appropriate dispersant is added to the dispersant unit, followed by a few drops of the sample. The degree of dilution is controlled by a variable called "obscuration," which can be monitored in real time as the sample is added to the dispersant, and after a short stabilization period for the sample and laser. Obscuration values may vary between 0.5% and 20%, depending on the sample, dilution, and the speed at which the dispersant is moved by the stirrer. As a result, it is imperative to develop a unique method for each sample to be analyzed, and new method development must be carried out when the sample's composition changes. Some users have the idea that on this instrument, parameters like obscuration or rpm should be kept constant regardless of the samples created (which migth vary on the amount of emulsifiers or the oils used for the emulsions). This is a mistake, as the theory used by the instrument has nothing to do with those parameters to report the correct size distribution.

Figure 18.7. A shows the result of a liquid measurement using an obscuration of ~10%. Note that the *X*-axis is in a logarithmic scale, making it easy to visualize many length scales simultaneously, while the *Y*-axis is the volume density %. Figure 18.7b is a histogram that emphasizes that this instrument measures size distributions, with the *Y*-axis now representing volume %.

In Fig. 18.7a, a wide distribution ranging from 0.1 to 1100 μm is observed, with three distinct modes in the data. The largest peak among the three modes is observed at ~30 μm. However, it is important to note that this does not mean that the majority of the particles are of this size, as the volume density is only around 5% and not 100%. To further characterize the particle size distribution, DLS users commonly use parameters such as D [3,2] (Surface Weighted Mean), D [4,3] (Volume Weighted Mean), or Dv10, Dv50, and Dv90. These last three parameters indicate the size below which 10 or 50 or 90% of the total particles exist, where the DvXX value represents the size. Interested readers can refer to the Mastersizer 3000 User Manual and User Guide for more detailed information.

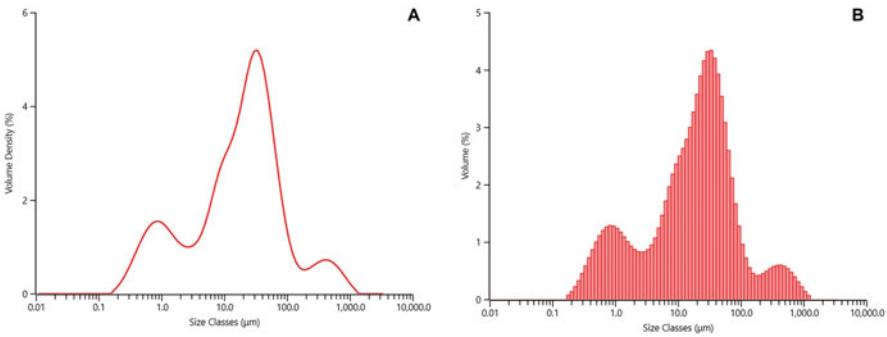

Fig. 18.7 Example of a particle size distribution obtained using a Malvern Mastersizer 3000. (**a**) Volume percentage as a function of particle size (size classes). (**b**) Histogram displaying volume percentage as a function of particle size. (*Source*: Courtesy of the Core Lab at the Food Science Department, University of Guelph, Canada)

Precisely quantifying oleogels using dynamic light scattering (DLS) systems poses challenges due to the inherent risk of disrupting the desired particulate structure during dispersion in the dispersant, potentially leading to their dissolution. As mentioned before, the DLS equipment necessitates the placement of droplets of the oleogel within a suitable dispersant, such as oil or water. However, this approach may compromise the accuracy of the measurements due to dilution effects of the oleogel under study. It is evident that DLS can serve as a suitable technique for quantifying oleogel-based emulsions or nano-emulsions, rather than directly assessing the properties of oleogels themselves.

Modern DLS instruments have the capability to measure powders, but the parameters required for introducing the sample into the equipment differ from those used for measuring liquids. To measure liquids, users must input values such as obscuration and RPM of the stirrer in the dispersant unit. However, when measuring powders, users must select the air pressure, tray feeding rate, obscuration, and hoper gap size.

Penalty Points

The DLS technique may require the use of an organic solvent for liquid measurements, which can result in penalty points (PP). When water is used, no PP is assigned for the chemical used. However, when ethanol is used, the PP is calculated as $2 \times (2 + 2) = 8$, as the dispersant unit can hold 100 mL of liquid, and ethanol has two pictograms and the "hazard" word. Nevertheless, since the measurement can be completed in a few minutes, the amount of electricity used is likely to be less than 1.5 kWh, resulting in a PP of 1. However, when using the powder technique, there are no penalties point due to reagents or chemicals. In this case, the only PPs are due to run the equipment and the vacuum machine that removes the powder, resulting in PP of 1.

Relevant Information Regarding the Technique

Spatial length scale	Operation of equipment ($, $$, $$$)	Parameters to measure	Penalty points
Nanometers to micrometers	$$	Particle size distribution q-vector vs. intensity	1–9 for liquids 1 for powders

18.2.7 Scanning and Transmission Electron Microscopy

Electron microscopy (EM), encompassing both scanning electron microscopy (SEM) and transmission electron microscopy (TEM), represents a powerful analytical technique that utilizes beams of electrons to illuminate samples for visualization and sizing of exceedingly small particles. Notably, at the nanoscale, a particle represents a collection of molecules, whereas at the micrometer scale, it may comprise an aggregation of particles of nanometer dimensions.

EM focuses an electron beam onto the sample, controlled by coils and apertures instead of glass lenses as used in light microscopy. The SEM scans the electron beam across the surface of the sample from top to bottom and from right to left, while the TEM transmits the beam through the sample. Both types of microscopies utilize an electron gun with an electron source, a Wehnelt cylinder, and an anode to form and accelerate the beam. When the electron beam interacts with the sample, it can be absorbed or diffracted by the atoms in the sample, creating secondary and backscattered electrons, X-rays, visible light, and heat. The SEM utilizes secondary and backscattered electrons for imaging, which show morphology and topography and illustrate contrasts in composition, respectively.

A cryogenic (Cryo) system used in conjunction with SEM improves the imaging when contrast is lacking at room temperature. The system preserves the internal structure of the sample by rapidly freezing it at liquid-nitrogen temperatures. The frozen sample is then transferred to a preparation chamber under vacuum conditions, where it undergoes manipulations such as cold fracturing, sublimation of surface ice, and nanometer-thick cadmium/gold coating. The fractured and coated sample is transferred to the SEM chamber for further analysis under cryogenic conditions. The constant −170 °C temperature is guaranteed by the Cryo system attached to the gun of the SEM. Overall, EM and its types provide powerful imaging techniques for visualizing and sizing particles at small scales, and the use of a Cryo system with SEM enhances imaging capabilities by preserving the internal structure of the sample.

The transmission electron microscope works by directing a beam of electrons through a thin film of the sample before capturing the image on a fluorescent screen for observation. It is critical to have a thin layer (around 100 nm) to prevent

excessive absorption of the electron beam by the material, which would prevent it from reaching the screen. This equipment takes advantage of the high speed of electrons; the faster they move, the shorter the wavelength and the greater the quality and detail of the image. The fluorescent screen shows light and dark areas, with lighter regions indicating where more electrons passed through the sample and darker areas representing denser regions. These differences provide valuable information on the sample's structure, texture, shape, and size. For certain samples, it is necessary to freeze them with liquid nitrogen to "fix" them and prevent changes over time.

What sets EM apart from light microscopy is its superior resolution. Resolution refers to the ability to distinguish two closely spaced points (particles) as two separate entities. EM can achieve resolutions between 0.2 and 0.05 nm, with the accelerating voltage being a key factor. In a scanning electron microscope, the accelerating voltage can range from 500 to 30,000 eV. Electrons accelerated by a potential of 30 keV have shorter wavelengths than those accelerated by 5 keV, resulting in better resolution for the 30 keV beam. TEM can handle voltages between 40 and 100 keV, offering even higher resolution than SEM.

Visualizing oleogels with SEM is challenging because the contrast between the oleogelator and the oil is not very distinct as can be seen in Fig. 18.8a. However, TEM offers higher resolution and allows for a clear identification of the features as seen in Fig. 18.8b. Proper sample preparation is crucial for successful observation using either technique. De-oiling is a useful preparation technique for visualizing oleogels. It involves removing the oil from the sample while keeping it at refrigeration temperatures to prevent melting of the desired components during observation. De-oiling can be accomplished using organic solvents [25–27] or soaps [28–30]. However, care must be taken during de-oiling, as it can lead to various issues that may affect the matrix of interest.

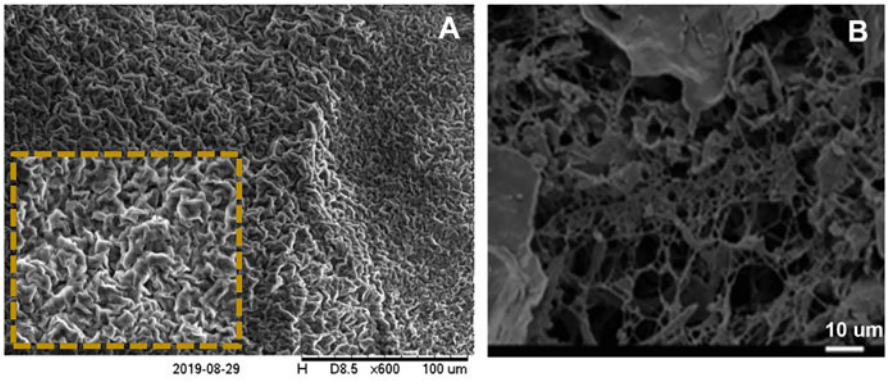

Fig. 18.8 Electron microscopy imagines of two oleogels. (**a**) SEM of an oleogel made using 10% berry wax in flaxseed oil. (Reproduced with permission from [31] under the terms and conditions of the Creative Commons Attribution License (CC BY)). (**b**) Cryo TEM of an oleogel made using 7% oleogelator (79% of fruit wax, Myrica cerifera with 21% soya lecithin) in sunflower oil. (Reproduced from [32], with permission from The Royal Society of Chemistry)

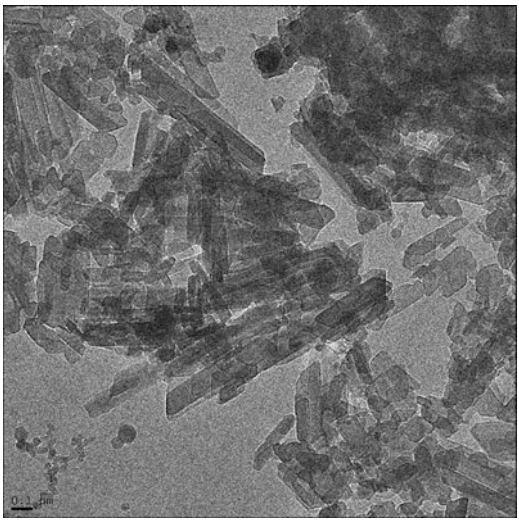

Fig. 18.9 Oleogelator particles. The oleogel was prepared using 20% tristearin in triolein. The cryo TEM image was obtained after de-oiling the oleogel to reveal only the olegelator basic unit. (Reproduced from Peyronel et al. [35] with permission from AIP Publishing)

TEM has been utilized in various systems, such as those where a hard fat is dispersed in a soft one [30, 33, 34]. For instance, Fig. 18.9 illustrates the case where nanoplatelets of tristearin (SSS) were de-oiled from triolein (OOO), the dispersant used in the oleogel. The preparation of the sample to obtain this image was crucial, as the OOO had to be entirely removed while preserving the desired particles to be observed from being destroyed in the de-oiling process [33, 35].

Over the past decade, advances in technology for data acquisition and software analysis have facilitated users to collect and process data without much consideration for the entire process. Generally, the data obtained from both SEM and TEM are ready for analysis. The software saves the scale with the captured photo, and users can measure the desired crystals if needed. The microscope software enables sample analysis, or users can take advantage of the many software options available on the market. One such popular free software is Image J. When performing crystal measurements, it is essential to define the crystal's boundary, which can be achieved by using a threshold that employs contrasting colors. A threshold is typically used when the user wants the software to measure and report automatically. Manual measurement may not be ideal, as the user must decide on the boundary for each crystal, which is challenging to do with the naked eye.

Penalties Points

Using SEM and TEM instruments incurs penalties points due to their high costs and energy consumption. These instruments are typically located in a central facility, and users pay to access and use them. Operating an electron microscope (EM) requires a considerable amount of energy to run the electron gun, mobile parts, and pumps to produce a vacuum. The energy consumption is typically greater than 1.5 kWh, resulting in a penalty point (PP) of 2. If Cryo is also used, there is an additional cost associated with the liquid nitrogen used, which is never less than 100 m. As

liquid nitrogen has a warning label, it incurs an additional PP of 2, resulting in a total of 4 PPs. Special glues, such as glutaraldehyde, may be required for SEM, which falls below 10 mL and incurs no penalty points.

Additionally, SEM requires argon and either cadmium or gold for sputter coating. Argon is dispensed at a low flow rate for 10–30 min, resulting in a reagent PP of 1 (between 10 and 100 mL). Argon has only one pictogram and no hazardous working in its label, resulting in a total PP of 1. Cadmium is used in very small amounts (less than 10 mL) and incurs no penalty points. Therefore, the PP for operating this instrument can range from 2 PPs to 7 PPs (2 + 0 + 4 + 1).

Relevant Information Regarding the Technique

Spatial length scale	Operation of equipment ($, $$, $$$)	Parameters to measure	Penalty points
Nanometers to micrometers	$$$	Crystal sizes Crystal morphologies	2–7

18.2.8 Confocal Microscopy

A confocal microscope uses a laser instead of electrons or visible light to create images. The laser is scanned across the sample to produce the image, with a narrower depth field than a traditional "wide field" light microscope. The name "confocal" comes from the fact that only information from the plane of focus is detected, achieved using a pinhole that cuts off signals that are out of focus. In addition to its narrow depth of field, the confocal microscope has several advantages, including its ability to resolve smaller details than a conventional light microscope (~100 nm) and its rapid image collection, which can be previewed before saving. The confocal microscope is particularly useful for obtaining three-dimensional images, as the focus plane can be repositioned, and the images stacked together.

To be analyzed with a confocal microscope, samples need to be fluorescent or reflective. The microscope is typically operated in epi-fluorescence mode, where the illuminated and emitted light travels through the same objective lens. This mode is particularly useful for imaging thick samples (over 10 μm deep). Fluorescence allows researchers to include stains that make molecules of interest fluoresce, allowing for the viewing of specific features in the sample. Multiple dyes can be used simultaneously to differentiate components in the sample. Most confocal microscopes have one or more lasers that can excite most common fluorescent probes using a mercury lamp (e.g., fluorescein-5-isothiocyanate (FTIC), rhodamines, and cyanine dyes), with UV lasers also available to excite probes such as 4′,6-diamidino-2-phenylindole or DAPI or Fura-2.

The reflected mode is used to image surfaces or reflective stains within samples, while the transmitted mode functions similarly to a conventional light microscope, allowing samples to be viewed by bright field, darkfield, phase contrast, or differential interference contrast. Some confocal manufacturers now support full color transmitted light imaging.

Results obtained from a confocal microscope can be interpreted similarly to any other microscope, including the size and shape of crystals, as well as the density of the crystals. Software is recommended for analysis, as the human eye may struggle to consistently distinguish between the crystal and background.

One group that took advantage of the reflection of the laser on needle-like crystals is Holey and colleagues [36]. They did not use any dyes and did not create 3D images by scanning at different focal points, resulting in a micrograph like what can be obtained from bright field. On the other hand, the gel made by Gu and coworkers [37] was a simple emulsion using 50% distilled water, 43.8%, soybean oil, 2.2% PGPR and 5% rice bran wax. The stirring was done at 90 °C before it was quickly cooled to 4 °C. Figure 18.10 shows confocal images of the above-mentioned gel. The authors had used Nile blue to stain the wax and Nile Red to stain the oil phase. It can be seen in Fig. 18.10 how easily one can distinguish one phase from another by using a different wavelength of the laser.

Penalties Points

There are some considerations to keep in mind when using a confocal microscope regarding the number of PP. While fluorescence typically requires staining, the amount needed is usually less than 10 mL, resulting in no PP. However, operating lasers does require a significant amount of power, with the Eco-scale indicating that the PPs = 2 for consumption over 1.5 kWh.

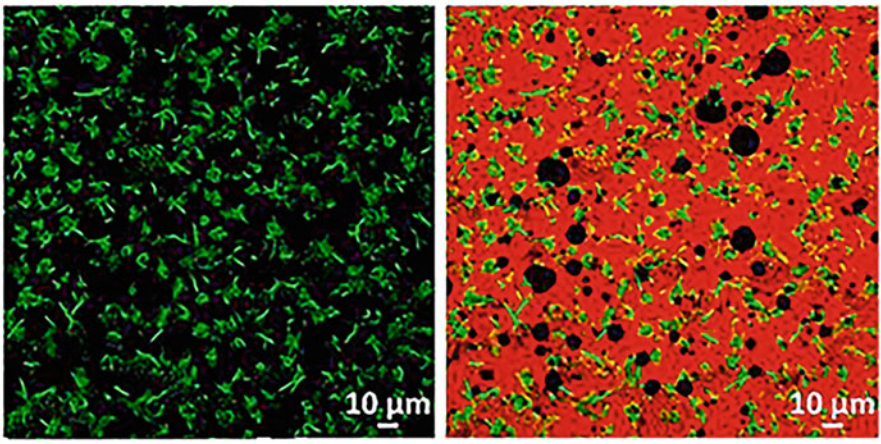

Fig. 18.10 Confocal images of a simple emulsion made using water, rice bran wax (green) and soybean oil (red droplets). The black droplets are believed to be water. (**a**) Fluorescence image of the wax crystals, (**b**) overlay fluorescence image of the oil phase and wax crystal using two different stains. (Reproduced from [37] with permission from Elsevier)

Relevant Information Regarding the Technique

Spatial length scale	Operation of equipment ($, $$, $$$)	Parameters to measure	Penalty points
Nanometers to micrometers	$$$	Crystal sizes Crystal morphologies	2

18.2.9 Atomic Force Microscopy

Atomic force spectroscopy (AFM) is a powerful tool used to detect structures of different stiffness buried within a sample, using stiffness tomography. Typically, an AFM instrument consists of an arm to which a cantilever is attached, with the cantilever chosen according to the material to be analyzed. The dimensions of the cantilever are typically in the scale of micrometers, while the radius of the tip is usually on the scale of a few nanometers to a few tens of nanometers. The atom at the apex of the tip "senses" individual atoms on the sample surface when it forms incipient chemical bonds with each atom. The system measures the forces between the chemical bonds obtained in an accurate and precise manner for each type of atom expected in the sample. A spatial map of the interactions is made by measuring the deflection at many points on a 2D surface. The beam-deflection method is popular due to its high sensitivity and simple operation, and because cantilevers can be fabricated relatively cheaply with sharp integrated tips, without requiring electrical contacts or other special treatments.

In a study conducted by Zetzl and coworkers [38], ethyl cellulose was utilized at two distinct viscosities in conjunction with either soya bean oil or canola oil, revealing the formation of a spongy structure through atomic force microscopy (AFM) analysis. However, the application of this technique posed certain challenges, primarily involving the effective removal of the oil without destroying the solid matrix to image, and the appropriate setup of the AFM instrument. To address these issues, the authors submerged the oleogel in isobutanol for a duration of 24 h, allowing for the subsequent collection of AFM images while the oleogel matrix remained immersed in water.

Penalties Points

It should be noted that if organic solvents are used in the sample preparation, there may be some penalties points (PP) associated with the technique. Equation (18.1) could be as simple as PP = 0, if the amount of solvent used is less than 10 mL, or it could become PP = 4 if between 10 and 100 mL of 2-propanol is used (2 pictograms and the word "hazard"). Additionally, an atomic force microscope is a sophisticated instrument with many different parts that require electricity to operate. Its consumption might be less than 1.5 kWh per hour or over it, hence the PP due to electricity consumption can be either 1 or 2. We have not included the penalties points (PP)

associated with cantilever preparation, but it should be noted that the fabrication process involves the use of chemicals, which may contribute to PP.

Relevant Information Regarding the Technique

Spatial length scale	Operation of equipment ($, $$, $$$)	Parameters to measure	Penalty points
Nanometers to micrometers	$$	Particle sizes	1–6

18.2.10 Pulse Nuclear Magnetic Resonance (NMR)

Nuclear magnetic resonance spectroscopy (NMR spectroscopy) or magnetic resonance spectroscopy (MRS) is a widely employed analytical technique utilized to investigate the local magnetic fields surrounding atomic nuclei. The technique relies on measuring the absorption of electromagnetic radiation in the radio frequency range spanning from ~4 to 900 MHz. The sample of interest is positioned within a magnetic field, and the NMR signal is generated by exciting the nuclei with radio waves, ultimately inducing nuclear magnetic resonance that is detected by highly sensitive radio receivers. The intramolecular magnetic field surrounding an atom in a molecule alters the resonance frequency, thereby enabling the elucidation of the electronic structure of a molecule and its individual functional groups. While a frequency of 900 MHz is suitable for exciting hydrogen nuclei, the nuclear magnetic moments of different nuclei vary, leading to distinct resonance frequencies that are proportional to the field strength [39].

NMR spectroscopy is a versatile analytical tool that comprises three fundamental steps: first, nuclear spins are aligned within a magnetic field; second, a radiofrequency (RF) pulse perturbs the nuclear spins; and third, the resulting NMR signal is detected either during or after the RF pulse. For the analysis of oleogels, pulsed nuclear magnetic resonance (pNMR) represents a preferred technique. Unlike traditional NMR instruments that require substantial equipment and infrastructure, pNMR is a benchtop instrument that is readily accessible to a wide range of researchers. While pNMR has long been utilized to measure the solid fat content (SFC) of edible fats [40], it also holds promise for the simultaneous determination of fat and water content [41] and for the analysis of gelled and bigelled emulsions, provided that the water concentration does not exceed 15% [42]. Notably, pNMR represents a non-destructive analytical technique that is well suited for the investigation of complex systems [43].

In the context of oleogel analysis, pNMR is commonly employed for the measurement of solid fat content (SFC). During pNMR analysis, the oleogel is subjected to electromagnetic excitation, which leads to interactions between liquid-state nuclei and the surrounding nuclei. The pNMR is a dedicated instrument that only induces protons, or hydrogens atom to go into an excited state and since uses pulses, as soon

as the pulse is removed, the hydrogen nuclei relax from their excited state. Solid-state hydrogen nuclei relax faster than the liquid-state hydrogen nuclei. The interaction of the nuclei is recorded as they relax in a curve called the Free Induction Decay (FID). The data from the FID enables the calculation of the number of solids-proton nuclei in the sample. This technique is particularly useful in analyzing oleogels due to the high number of hydrogen atoms present in almost all the molecules. A compound present in the liquid phase will retain its full diffusive mobility, while a constituent of a crystal or polymeric network will be substantially immobilized within the gel matrix. The percentage of solid matter in the system, referred to as the solids content, is commonly used to express the amount of solid content in the sample. By employing this method, researchers can accurately determine the solids content and assess the performance of oleogels in various applications.

Over the years, various standardized methods have been established to measure the SFC, including the AOCS direct method Cd 16b-93 [44], AOCS indirect method Cd 16–81 [45], as well as international standards such as ISO 8292 and IUPAC 2.150. These methods provide users with reliable and reproducible means of measuring SFC in order to ensure consistency and accuracy in the assessment of edible fats. These measurements are typically conducted using benchtop equipment, such as the one illustrated in Fig. 18.11a, which must be calibrated prior to use. This assessment is performed after oleogels have been formed and involves a storage period at a predetermined temperature to evaluate the effect of the gelator on structuring development. The oleogel can be directly placed in the sample container for measurement or molten oleogel can be poured into the container and subjected to a preset program that may include agitation and temperature control, as shown in Fig. 18.11b–e. To obtain precise and reproducible measurements, it is essential to comply with the recommended amount or height of the sample in the container specified by the equipment supplier. To ensure accuracy, it is advisable to allow a minimum of 24 h at the structuring temperature before taking measurements and to stabilize the oleogel for at least 1 h at the temperature designated for the measurement of SFC.

To facilitate thermal treatment of the oil sample for the purpose of structuring it prior to performing the SFC measurement, a variety of heating media can be employed, as depicted in Fig. 18.11b–e, contingent upon the specific experimental configuration. The reading on the equipment is obtained by directly inserting the tube containing the oleogel into the compartment of the resonance equipment. For this analysis, it is recommended to perform three to five measurements per sample to ensure accuracy and reproducibility.

Figure 18.12a displays the SFC as a function of temperature for palm olein, palm stearin, three of their mixtures and beeswax, which are materials commonly used to make oleogels. On the other hand, Fig. 18.12b shows that the amount of beeswax has an important impact on the SFC profile. The more beeswax used, the higher the SFC, no matter which blend of olein/stearin was studied.

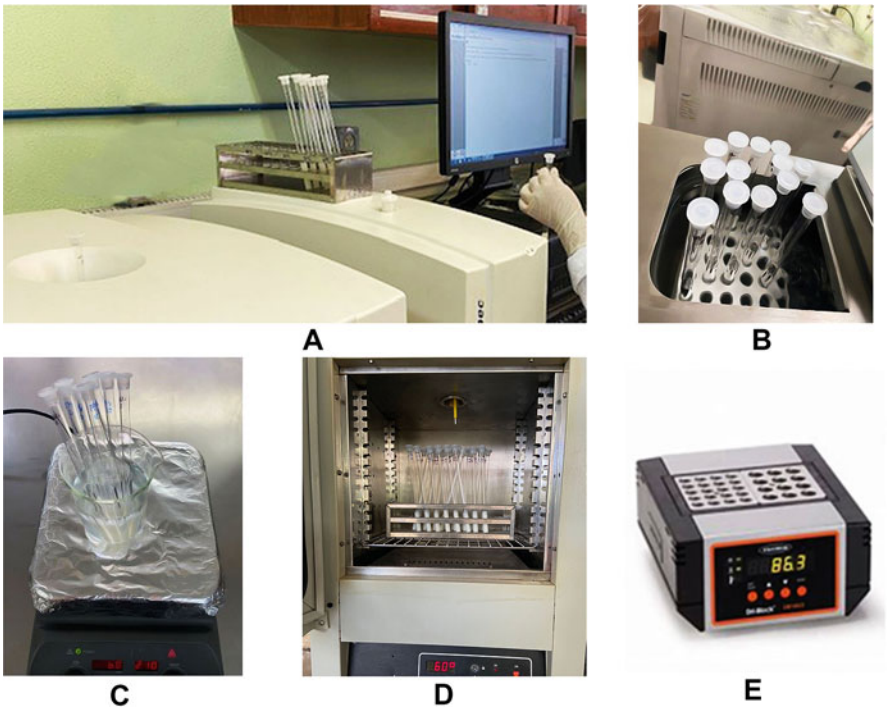

Fig. 18.11 Pulse nuclear magnetic resonance analyzer unit (**a**). Glass tubes in: a water bath (**b**), hot plate (**c**), electrical oven (**d**) and a dry heater (**e**). (*Source*: Courtesy of Food Biopolymer Lab, Faculty of Chemical Sciences of the Autonomous University of San Luis Potosí, except (**e**) (Techne Dri-block))

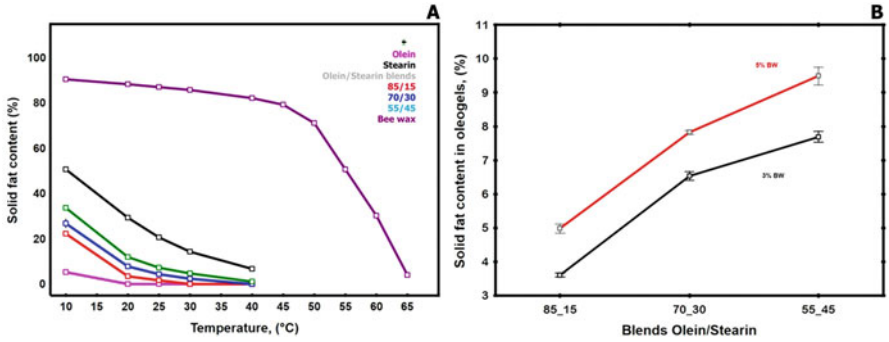

Fig. 18.12 Solid fat content of individual and mixed oils and beeswax. (**a**) Palm oil olein, palm stearin, their mixtures (85/15, 70/30, 55/45 – olein/stearin-) and beeswax. (**b**) 3% and 5% beeswax added to mixtures of olein/stearin (85/15, 70/30, 55/45). (*Source*: Courtesy of Food Biopolymer Lab, Faculty of Chemical Sciences of the Autonomous University of San Luis Potosí)

Penalties Points

This technique uses pNMR equipment to measure the SFC and does not require the use of reagents or solvents. There are two sources of electricity consumption: the first comes from the temperature profile that the sample must undergo, and the second comes from the use of the equipment required for measuring the SFC. The pNMR equipment only requires energy to generate resonance and to apply it in the oleogel. Typically, a pNMR equipment consumes less than 1.5 kWh of energy, hence resulting in PP = 1. When carrying out the AOCS protocol for the SFC measurement, 5 water baths are needed, the PP for each of them is 0, but since there are five, it could be considered a PP = 1. Thus, the total PPs required for this process could be as much as 2.

Relevant Information Regarding the Technique

Spatial Length Scale	Operation of Equipment ($, $$, $$$)	Parameters to Measure	Penalty Points
Millimeters	$$$	Solid fat content Fat solids content curves Total fat and water content in oleogel emulsion	1–2

18.3 Chemical Characterization

18.3.1 Raman Spectroscopy

Raman spectroscopy involves shining a monochromatic laser beam of light on a sample, which can be absorbed, transmitted, reflected, or scattered. This technique is concerned with inelastic scattering, which deals with different frequencies associated with the vibrational frequencies of the molecules in the sample. Although Raman scattering is about a million times less intense than elastic (Rayleigh) scattering, it provides valuable information about the sample. The Raman shift is the energy difference between the incident light and the Raman scattered light, and the resulting spectrum shows the intensity of the scattered light on the vertical axis and the Raman shift on the horizontal axis. The Raman shift can be either above the incident laser frequency (Stokes scattering) or below (anti-Stokes scattering). Additionally, Rayleigh scattering is a sharp, strong peak located between the Stokes and anti-Stokes peaks. In Raman spectroscopy, the intensity of the scattered light depends on the degree of polarizability (electron volume) for vibration modes for bonds such as S−S, C−C, and total carbon number (CN). This technique is also sensitive to homonuclear molecular bonds such as C−C, C=C, and C≡C bonds.

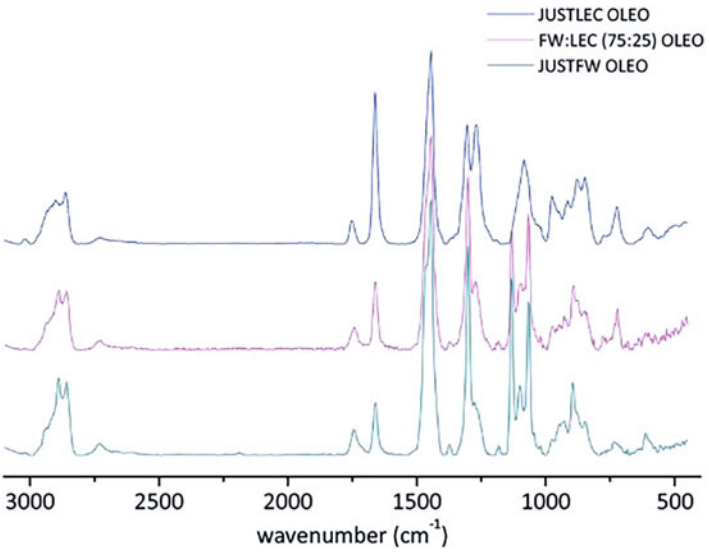

Fig. 18.13 Raman spectrum of lecithin (JUSTLEC OLEO), the mixtures of fruit wax and lecithin (FW:LEC 75:25 OLEO) and fruit wax (JUST FW OLEO). (Reproduced from [32], with permission from The Royal Society of Chemistry)

For example, in a study by Okuro and colleagues [32] Raman spectra of two oleogelators used in sunflower oil were analyzed. The oleogelators were fruit waxes (FW) and soya lecithin (LEC), and changes in the shape and frequency of the molecular vibrations' bands were monitored to explain possible interactions. The authors observed peaks at 3021 and 720 cm^{-1} in lecithin oleogels, which correspond to the asymmetric stretching vibrations of the choline head group and the C-N stretching, respectively. The asymmetric CH_2 stretching mode was 2899 and 2889 cm^{-1} for LEC and FW, respectively. When LEC and FW were mixed, the authors observed a peak at 2886 cm^{-1}. They also found that the symmetric CH_2 stretching mode was the same for both single-component oleogels (2858 cm^{-1}) but shifted to 2860 cm^{-1} in the mixture (Fig. 18.13).

Penalty Points

Although there is no sample preparation for this technique, the equipment itself requires large amounts of electrical power (more than 1.5 kWh), resulting in two penalty points.

Relevant Information Regarding the Technique

Spatial length scale	Operation of equipment ($, $$, $$$)	Parameters to measure	Penalty points
Atomic scale	$$$	Bonds between atoms	2

18.3.2 Fourier Transform Infrared (FTIR) Spectroscopy

Fourier transform spectroscopy is a powerful analytical technique that enables the simultaneous detection of all wavelengths of infrared light transmitted or reflected by a sample. Rather than scattering, the technique relies on the detection of interference. When the sample is irradiated with infrared radiation, the covalent bonds within its molecules get excited, producing vibrations that include stretching and bending modes. The absorbed wavelength of light is a function of the energy difference between the at-rest and the excited vibrational states. Fourier transform infrared (FTIR) spectroscopy uses an interferometer to modulate the wavelength of light from a broadband infrared source. The signal detected by the instrument is an interferogram, which is then analyzed using Fourier transforms to obtain a single-beam infrared spectrum. The resulting FTIR spectra are usually presented as plots of intensity versus wavenumber (cm^{-1}), where wavenumber is the reciprocal of the wavelength. The intensity can be plotted as either the percentage of light transmittance or absorbance at each wavenumber.

FTIR analysis provides valuable information for material identification by identifying molecular components and structures. The absorption peaks in the fingerprint region (Region 2, $<1000\ cm^{-1}$) are unique to each molecule and can be compared to known standards for identification. However, the fingerprint region is complex, and assigning peaks can be challenging. The functional group region (Region 1, 1000–4000 cm^{-1}) is the most informative and contains peaks that correspond to specific functional groups. Polar covalent bonds are IR active, indicating that they will absorb in the IR spectrum. IR spectroscopy is sensitive to heteronuclear functional group vibrations and polar bonds, such as OH stretching in water. The intensity of the spectral absorption depends on the size of the dipole moment for vibration modes for bonds such as C=O and O−H. Some functional groups can be "viewed" as combinations of different bond types. For example, an ester (CO_2R) contains both C=O and C−O bonds, which are typically seen in an IR spectrum of an ester.

FTIR analysis can be a qualitative tool for material identification, but it can also be used as a quantitative tool to quantify specific functional groups when standard reference materials and a good understanding of the chemistry are available. The intensity of the absorbance correlates with the quantity of "functional groups" present in the sample. However, the presence of other chemical and matrix factors can cause the peak position to shift. Lookup tables for IR spectra can be found in the literature, but they are limited in scope and depth compared to the millions of industrial chemicals available. As a result, researchers often rely on previous research in the same area to identify bands.

Figure 18.14 shows an FTIR spectrum of an oleogel made with a mixture of β-sitosterol and beeswax as the oleogelator in sunflower oil [46]. The fingerprint region of the spectrum reveals significant differences in the position of peaks when the β-sitosterol and beeswax are separated. The peak at 1460 cm^{-1} corresponds to the −OH bending, while the peak at 1170 cm^{-1} is associated with the –CO

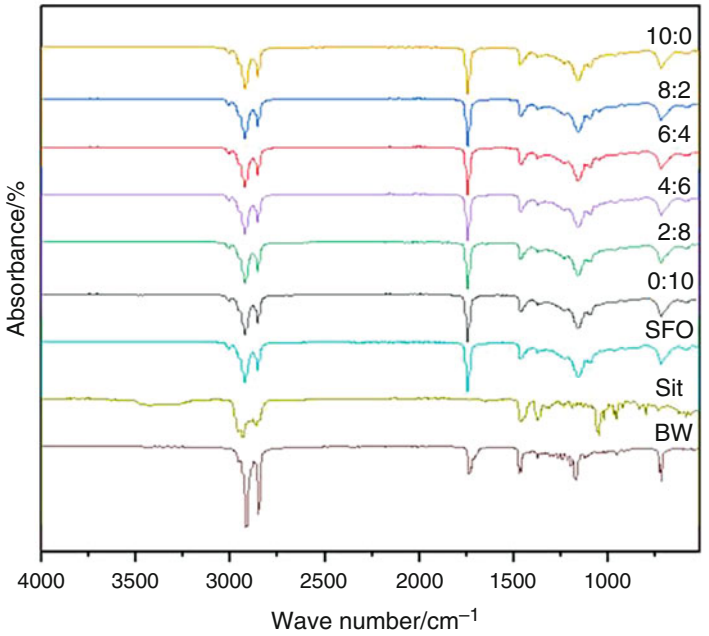

Fig. 18.14 FTIR spectra of two oleogelators (Beeswax, BW, and β-sitosterol, SIT), the oil (sunflower SFO) used to make the oleogel and six different mixtures of oleogelators (SIT:BW). The oleogels contained 10% of the mix of oleogelators, (0:10, 2:8, 4:6, 6:4, 8:2, 10:0). (Reproduced from [46] with permission from John Wiley and Sons)

stretching. In contrast, there is little difference among the oleogels in the functional group region. Both β-sitosterol and beeswax show peaks in the C−H stretching region (2800–3000 cm^{-1}). The FTIR results shown in Fig. 18.14 suggest that the oleogels made with mixtures of β-sitosterol and beeswax were not formed by creating new covalent bonds.

Penalty Points

It should be noted that the FTIR instrument used for this analysis requires a significant amount of electrical power, as it uses a laser in the microscope. As a result, it is considered to be a high-power instrument, with PPs = 2.

Relevant Information Regarding the Technique

Spatial length scale	Operation of equipment ($, $$, $$$)	Parameters to measure	Penalty points
Atomic scale	$$$	Characterize elements and functional groups	2

18.3.3 Gas Chromatography

Gas chromatography (GC) is a powerful analytical separation technique used for the separating volatile compounds present in a gas phase. The technique can be applied to samples that are either in the gas phase or require prior derivatization and pyrolysis. A gaseous sample is injected onto the head of a chromatographic column, which is typically several meters long and filled with a stationary phase. Elution of the analytes in the samples is brought about by the flow of an inert gaseous mobile phase such as helium, argon, nitrogen, carbon dioxide, and hydrogen. The stationary phase can either be a solid adsorbent (GSC, gas-solid chromatography) or a liquid immobilized on an inert support (GLC, gas-liquid chromatography), with the latter being the more commonly used technique. Separation of analytes is achieved based on their relative vapor pressures and affinities to the stationary phase [47]. Hence, the choice of column is critical, as it significantly impacts the separation of analytes. Samples are usually not suitable for direct introduction into the GC instrument. It is crucial to refer to the literature for optimal sample preparation protocols.

Despite its origins in the separation of amino acids in 1950, gas chromatography has since become a widely utilized technique due to its high sensitivity, precision, and accuracy, as well as its ability to operate at fast rates and with small sample sizes (about few milligrams). To apply this technique, the sample must be volatile and heat stable [48] which permits the separation and analysis of the vegetable oils that comprise oleogels through GC, allowing for the determination of their respective fatty acid and triacylglycerides profile.

In order to determine the fatty acid (FA) profile in the oily phase of an oleogel (pure or blended vegetable oil), it is imperative to first derivatize the oily phase to separate the FAs from the glycerol molecule [49], wherein the FA will dissolve in the organic solvent employed. On the other hand, to quantify the triacylglyceride (TAG) profile of the oleogel oily phase, the sample should be dissolved solely in a solvent compatible with the column to be used [50]. The prepared sample is introduced into the chromatographer via the injection port, using a microsyringe to dispense the desired amount into the vaporization chamber. The majority of commercial gas chromatographs support injection in two modalities: split or divided injections, which utilize a sample divider to direct excess sample to waste and splitless or without division injections. The vaporization chamber is typically heated to 50 °C above the lowest boiling point of the analytes present in the sample. The vaporized sample is mixed with the carrier gas at the head of the column and transported through the column.

To ensure accuracy and reproducibility in the determination, process, precise control of the column temperature is essential. The column temperature is controlled using an equipment oven, which can operate in either isothermal programming where the column temperature is maintained constant throughout the separation, or temperature programming, where the column temperature is increased continuously or in steps as the separation progresses. The rates of temperature increase during temperature ramps can vary depending on the elution interval of the fatty acids in the

column utilized [47]. Additionally, multidimensional gas chromatography (MDGC/GCxGC) is now available as a chromatography method for separating complex samples with components that have similar retention times. This technique involves passing the eluent through two or more columns, as opposed to the traditional single column approach.

The outlet of the GC column is the detector, which captures data as intensity over time. Several types of detectors are commonly used in GC, including the flame ionization detector, mass spectrometer (MS), electron capture detector (ECD), thermal conductivity detector (TCD), and atomic emission detector (AED), among others. The flame ionization detector and mass spectrometer are the most employed detectors for separating fatty acids. The GC software records the raw data as a chromatogram, which can be further processed by the user. The chromatogram displays peaks at specific elution times, corresponding to the retention times of the analytes present in the sample. For instance, In the case of FAs in the oily phase of an oleogel, the retention time is dependent on the length of the hydrocarbon chain and degree of unsaturation of each FA. In a well-resolved sample, the number of analytes is equivalent to the number of peaks observed, and the relative abundance of each component is represented by the area under the curve of each peak relative to the total area [47]. If standards are used, absolute quantification can be performed for each of peaks corresponding to each analyte. To compliment this methodology, the official methods of the AOCS can be consulted [51, 52], or published works on the quantification of short-chain, unsaturated and *trans* fatty acids [53, 54].

Oleogels are commonly produced using unsaturated oils as solvent [55]. To demonstrate the application of this technique, we present the FA chromatogram of avocado oil in Fig. 18.15. Chromatography was performed using a flame ionization detector, with the injector temperature maintained between 220 and 250 °C and the

FATTY ACID (FA)	COMPOSITION IN AVOCADO OIL (%, w/w)
Palmitic, C16:0	14.96 (0.24)*
Palmitoleic, C16:1	5.52 (0.04)
Stearic, C18:0	0.72 (0.03)
Oleic, C18:1c	59.58 (0.76)
Oleic, C18:1c	5.03 (0.12)
Linoleic, C18:2	13.24 (0.45)
Linolenic, C18:3	0.95 (0.01)
FA Saturated	15.68 (0.24)
FA Insaturated	84.32 (0.76)
-Monounsaturated	70.13 (0.76)
-Polyunsaturated	14.19 (0.45)
-Trans	0.00 (0.00)
* Mean and (standard deviation), n=4	

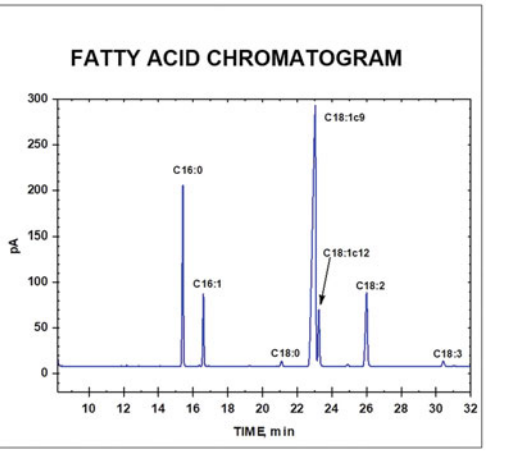

Fig. 18.15 Fatty acid profile and chromatogram obtained by gas chromatography of avocado oil used in an oleogel formulation. (*Source*: Courtesy of Food Biopolymer Lab, Faculty of Chemical Sciences of the Autonomous University of San Luis Potosí)

PRINCIPAL TAGs	COMPOSITION IN AVOCADO OIL (%, w/w)
POP	2.89 (0.00)*
POPo	7.14 (0.00)
PLPo	2.42 (0.06)
POO	18.24 (0.06)
POL	14.77 (0.02)
PLL	3.78 (0.00)
SOO	1.33 (0.05)
OOO	33.96 (0.32)
OLO/OOL	8.63 (0.12)
OLL/LOL	1.60 (0.12)

*Mean and (Standard Deviation), n=4.

P: Palmitic, Po: Palmitoleic, S: Stearic, O: Oleic, L: Linoleic

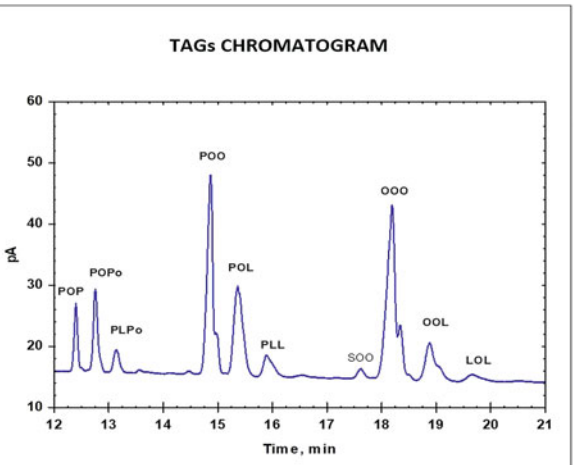

Fig. 18.16 Main triacylglycerides (TAGs) in avocado oil, which were analyzed by gas chromatography and the corresponding chromatogram. (*Source*: Courtesy of Food Biopolymer Lab, Faculty of Chemical Sciences of the Autonomous University of San Luis Potosí)

detector temperature around 250–270 °C. The AOCS official method [49] was utilized for derivatization, and separation was conducted using capillary columns. Recently, long-length capillary columns (90 at 100 m) have become available on the market, allowing for the separation of omega-3 and -6 FAs, as well as *cis* and *trans* isomers of FA methyl ester, which are typically found in oleogels. The use of high efficiency column may significantly reduce the analysis time (≈10 min vs. ≈50 min). The chromatograph for avocado oil was obtained using a cyanopropyl siloxane-based stationary phases with a recommended temperature of 180 °C. One or more temperature ramps can be employed to increase the temperature to values of 210 °C or higher, aiding in separation. A split mode injection of 100:1 or 50:1 ratio with helium as the carrier gas provided good resolution; we used a 100:1 ratio and a 1 μL injected sample volume. FA methyl esters were identified by comparing their retention times to those of FA standards analyzed under the same conditions as the sample and were quantified as a percentage of the area of the corresponding peak with respect to the sum of the areas of all peaks. Additionally, calibration curves may be created for specific analytes.

The physical structure of oleogels can be influenced by the composition of TAGs and their interaction with the oleogelator, as noted by Van Bockstaele and colleagues [56] TAGs have a more complex chemical structure than FAs, necessitating higher temperatures for their volatilization. The composition of TAGs can be determined via GC using the AOCS Ce 5–86 method [57]. Briefly, this technique involves a phenyl-methyl-polysiloxane-based capillary column with a length of 30 m, internal diameter of 0.32 mm, and a stationary phase thickness of 0.15 μm. The column temperature starts at 200 °C and is increased in two heating ramps to 300 °C at 25 °

C/min and to 350 °C at 30 °C/min. Helium is utilized as a carrier gas with a flow rate of 1.36 mL/min, while the injector and detector temperatures are set to 360 and 370 °C, respectively. The samples are dissolved in chloroform (10 mg/mL) and injected in split mode (50:1), with 1 μL of this solution.

The manufacturer of the chromatographer (e.g., ChemStation MSD from Agilent Technology) provides software that is utilized for data analysis. The peaks are identified based on the CN, excluding glycerol carbons, and their confirmation is done by analyzing commercial standards under identical conditions as the sample. The retention time of each peak directly corresponds to the CN, as shown in the chromatogram. In cases where there is the presence of TAG with the same CN, the carbon equivalent number can also be calculated [58]. Figure 18.16 presents the TAGs profile found in the avocado oil used to obtain the FA profile. The predominant TAGs consist of unsaturated hydrocarbon chains, which aligns with the FA findings. GC chromatography can also be employed to investigate the chemical profiles of waxes and gums, as noted by Doan and colleagues [59]. This method therefore offers a comprehensive understanding of the composition of oleogels, waxes, and gums, which can be valuable in various applications.

Penalties Points

The GC technique involves the use of solvents and reagents for sample derivatization, which can result in the imposition of penalty points (PPs). The PPs associated with the organic solvents and reagents used range from 4 to 13. Furthermore, the maintenance of the GC detector flame necessitates the continuous flow of nitrogen, helium, hydrogen, and air gases, resulting in an additional 2 PPs for gas consumption. The electricity consumption of a GC instrument, which exceeds 1.5 kWh, contributes an extra 2 PPs. The environmental impact of these PPs must be considered while assessing the sustainability of the GC technique.

Relevant Information Regarding the Technique

Spatial length scale	Operation of equipment ($, $$, $$$)	Parameters to measure	Penalty points
Atomic scale	$$ to $$$	Molecules identification	8–17

18.3.4 High-Pressure Liquid Chromatography (HPLC)

The High-Pressure Liquid Chromatography (HPLC) is a powerful tool for separating substances that are in suspension. The HPLC system works by utilizing the polarity differences of the eluent fluids (mobile phase) and the packing material (stationary phase) in the column to separate the compounds (analytes) in the sample. The equipment mixes the eluent with the analyte and pumps it under pressure through the column. The specific intermolecular interaction between the analyte and the stationary phase causes different molecules in the analyte to be retained inside

the column for different lengths of time. This results in the different components of the analyte being eluted at different times and shown on the signal captured by the detector (chromatogram).

A signal versus time chromatogram shows characteristic peaks that correspond to the different analytes present in the sample. The peaks should be separated from each other, and this is achieved by selecting the right mobile and stationary phase as well as the eluents and the conditions of operation of the HPLC. Depending on the composition of the mobile phase, two different modes are generally applicable. If the makeup of the mobile phase remains constant during the separation process, the HPLC system is defined as an isocratic elution system. When the composition of the mobile phase is changed during the process, the HPLC system is defined as a gradient elution system.

The column is the heart of any HPLC system and is designed specifically to separate certain compounds. The column's efficiency correlates with its inner diameter, length, and type and particle size of the packing material. Different packing materials support different separation mechanisms, including normal-phase, reversed-phase, size exclusion, ion exchange, affinity, chiral, or hydrophilic interaction HPLC.

As the analyte is eluted, the detector registers the time and amount of a substance that is eluted from the column. The detector perceives the change in the composition of the eluent and converts this information into an electrical signal, which is evaluated by the aid of a computer. Different detector units, such as refractometric, UV/VIS, electrochemical, and fluorescence detectors, have been used to identify different compounds. Each individual peak detected provides qualitative and quantitative information for the analyte. The area of a peak is proportional to the concentration of the substance.

The chromatography data management software can calculate the concentration of the sample by integration after standards are run. This requires a calibration curve, which nowadays, the data management software can handle easily and efficiently. Quantitative information can then be obtained. Ideally, the peaks are recorded as a Gaussian bell-shaped curve.

The HPLC technique is highly useful for analyzing oleogels in order to determine the compounds that constitute the oil and oleogelator. Proper sample preparation is of utmost importance and requires the sample to be in solution. Edible oils contain TAGs as their main components, but minor components must also be considered to ensure accurate results. When analyzing complex systems like oleogels using HPLC, it is crucial to select an appropriate eluent for each molecule (oleogelators vs. oil phase) to avoid misinterpretation of the results. Reversed-phase HPLC is commonly used for analyzing TAGs in oils and fats [60]. Various detectors have been utilized for TAGs identification, such as ultraviolet (UV) refractive index [61], evaporative light scattering detector [62–64] and mass spectrometry [65, 66]. Regio-isomers of TAGs have been examined in vegetable oils using atmospheric chemical ionization (APCI) mass spectrometry [60, 63, 65, 67]. The positional distribution of fatty acyl chains of TAG has been analyzed in palm oil, cocoa butter, beef, pork, and chicken

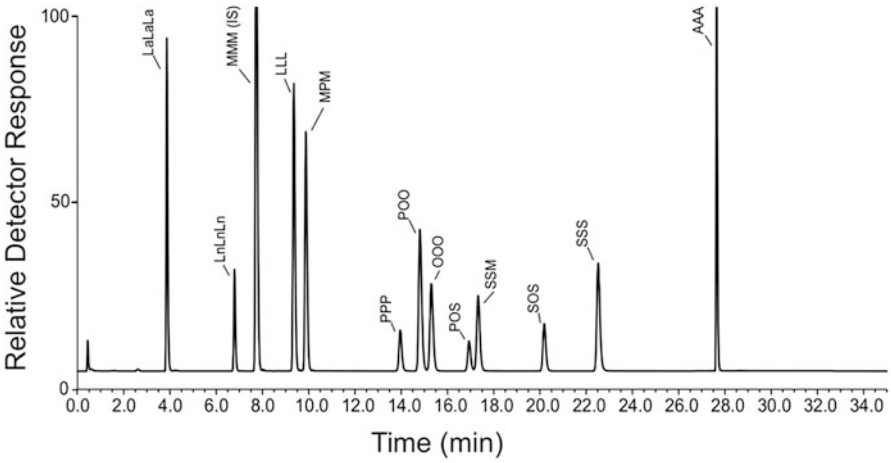

Fig. 18.17 UPLC-ELSD chromatogram of a mix of triacylglyceride (TAG) standards. Where the peaks correspond to the following TAGs: Triolein (OOO), trilaurin (LaLaLa), trilinolenin (LnLnLn), trilinolein (LLL), tripalmitin (PPP), tristearin (SSS), triarachidion (AAA), trimyristin (MMM), 1-pal-mito, 2,3-olein (POO), 1-palmito, 2-oleo, 3-stearin (POS), 1,2-stearo, 3-myristin (SSM), and 1,3-myristo, 2-palmitin (MPM). (Reproduced from [68] with permission from John Wiley and Sons)

fats using HPLC-APCI-MS. Individual regio-isomers were identified and quantified by linear calibration against the standards [65].

Figure 18.17 displays the peaks of some TAGs run on a reversed-phase liquid chromatography coupled with an evaporative light scattering detection (ELSD) by Ross and colleagues [68]. The authors utilized an Agilent Zorbax C18-XDB (100 mm, 62.1 mm, 1.8 μm) C18 column heated to 55 °C with a flow rate of 0.5 mL/min and an injection volume of 1 μL. Methanol and acetone were used as mobile phases, and a gradient was employed to elute the prepared standards using a sample that took 35 min in total. The molecules utilized for standards (samples) were prepared in dilutions of OOO in CH_3Cl_2 and $MeCl_2$ containing approximately 0.7 mg/mL of trimyristin (MMM) as the internal standard. Samples were prepared at a concentration of approximately 5 mg/mL by dissolving oils or fats in the CH_2Cl_2 internal standard solution.

It is important to note that Fig. 18.17 is just one example of how TAGs can be detected, and the resolution and ability to detect separate peaks depend not only on the HPLC but also on the detector. Mass spectrometry coupled with HPLC is a powerful technique that can help identify compounds that are difficult to separate into different peaks.

Penalties Points

The use of an HPLC incurs penalties points due to the solvents required for sample preparation and elution into the column. The Eco-Scale categorizes solvent use into three categories: less than 10 mL, 10–100 mL, and more than 100 mL. However,

running an HPLC requires equilibration and continuous elution of the analyte, so the amount of solvent used is typically over 100 mL. Organic solvents are not considered "good solvents," with two to four pictograms and either the "warning" or "hazard" word. Therefore, penalties points from one organic solvent can range from 2 to 6 PPs in the lower bracket and can increase to 6–18 PPs when a combination of solvents is used. Additionally, the electricity usage of an HPLC is greater than 1.5 kWh, resulting in the addition of 2 PPs due to electricity usage.

Relevant Information Regarding the Technique

Spatial length scale	Operation of equipment ($, $$, $$$)	Parameters to measure	Penalty points
Atomic scale	$$$	Molecules identification	8–20

18.3.5 Oxidative Stability

The oxidation of unsaturated fats is a well-established phenomenon that contributes to the deteriorations of oleogels. Fu and collaborators [69] have demonstrated that oleogels can undergo oxidative degradation due to their high content of unsaturated FAs from oils. This oxidative process can lead to undesirable changes in the aroma, color, and flavor of the product, as well as the loss of certain nutrients. Moreover, the formation of potentially harmful substances can further compromise the safety of the oleogels, ultimately resulting in a shortened shelf life. The economic implications of this phenomenon are significant, as it renders the affected oleogels unsuitable for consumption. Therefore, the scientific community must focus on developing effective strategies to prevent and mitigate this type of degradation. The economic implications of this phenomenon are significant, as it renders the affected oleogels unsuitable for consumption. Therefore, the scientific community must focus on developing effective strategies to prevent and mitigate this type of degradation.

Lipolysis or hydrolytic rancidity can occur in lipids due to the activity of lipases present in oils. However, the primary mode of lipid oxidation is initiated through a free radical chain propagation reaction, which involves the formation of peroxides and hydroperoxides from fatty acids and oxygen, known as auto-oxidation [70]. These compounds are highly unstable and can readily undergo breakdown, generating additional free radicals and perpetuating the oxidation process through a chain mechanism involving three distinct phases.

The induction phase is initiated by external factors such as light, heat, and trace heavy metals, which trigger the formation of peroxides and radical species. In the propagation phase, the oxidation of free radicals results in the formation of additional hydroperoxides and free radicals, which in turn participate in the oxidation chain. Ultimately, in the end phase, the concentration of reactive compounds reaches a critical threshold, triggering their interaction with one another and leading to the

formation of deteriorated products. The concentration of peroxide radicals diminishes as the formation of degraded products reaches a state of equilibrium, ultimately leading to a significant reduction in the quality and shelf life of lipids.

The oxidative stability of oleogels can be assessed by evaluating their oxidation level as a function of temperature and storage time. Chemical measurement of oxidation involves the quantification of compounds generated during the oxidation process, including peroxides, aldehydes, and ketones. Several methods are available for this purpose, including thiobarbituric acid, p-anisidine value, the amount of free fatty acid or conjugated dienes, and analysis of volatile oxidation products. Among these methods, peroxide quantification is commonly used to assess oxidation in oleogels [19, 69]. The peroxide value (PV) is expressed in milliequivalents or mmol of active oxygen per kilogram of lipid and measures the initial oxidation state of an oil. The American Oil Chemists' Society (AOCS) and the International Union of Pure and Applied Chemistry (IUPAC) offer standard procedures for this assessment.

Recently, VerraGlo LLC and the University of Kentucky collaborated [71] to develop patented foundational technology for metal-phosphate luminophores (MPL) sensors with peroxidase-like activity. These sensors emit luminescence proportional to the hydroperoxide content of edible fats and oils, offering a novel technique for peroxide value measurement that does not use or generate toxic solvents. This technique is abbreviated as PV-LED (Peroxide value light emitting diode) and has several advantages over traditional methods of peroxide quantification.

Regarding PV, Cho and colleagues [19] monitored the oxidation state of edible rice bran wax-gelatin biphasic gels for 175 days and found no significant changes in PV (between 0.17 and 2.62 mEq/kg), even in biphasic gels added with Cu2+ as a pro-oxidant agent. Giacomozzi and colleagues [72] also measured PV to study the storage stability of oleogels made from monoglycerides and high oleic sunflower oil, and similarly did not find significant changes in PV. However, Fu and colleagues [69] studied the thermo-oxidative behavior of ethyl cellulose oleogels and found that the presence of the gelling agent ethyl cellulose interfered with the reagents used in the determination of PV (KOH and $Na_2S_2O_3$), making this test inefficient and lowering the p-Anisidine value for evaluating the oxidation of oleogels. In a critical review of oleogels including oxidation, Park and Maleky [73] concluded that the oxidative stability of oleogels requires further research, particularly concerning the lack of information on the oxidative stability of foods formulated with oleogel and the effect of antioxidants in oleogel foods.

When evaluating the oxidation behavior of oleogels during shelf life, it is not only important to quantify the oxidation products present but also to predict the oxidative stability as a function of storage time through accelerated tests. There are various types of lipid analyses to predict this stability, with the most common being the active oxygen method (AOM) and the oxidative stability index (OSI) or Rancimat method [74], which expose the sample to increased temperature and elevated oxygen pressure. The AOM method, which was introduced in 1933, was the most widely used method for several years. O'Keefe and colleagues [75] used this method to compare the oxidative stability of peanut oil with high and normal oleic acid content. The AOCS officially adopted the AOM method under reference Cd 12–57 [76]. This

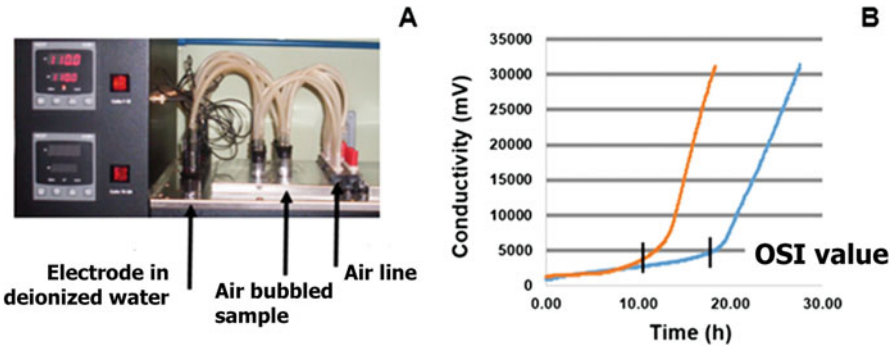

Fig. 18.18 Oxidative stability: (**a**) arrangement of elements in the instrument and (**b**) conductivity results as shown by the instrument for two vegetable oil samples indicating the oxidative stability index (OSI) value. (*Source*: Courtesy of Food Biopolymer Lab, Faculty of Chemical Sciences of the Autonomous University of San Luis Potosí)

method involves monitoring the peroxide index evolution in a sample subjected to the passage of an air current at a temperature of 97.8 °C. The stability of the sample is determined as the time required for the fat to reach a peroxide value (PV) of 100 mEq oxygen/kg lipid or, in some cases, to reach a PV of 10 mEq oxygen/kg lipid, which is the value at which the rancidity of the product is perceived. The OSI or Rancimat method is a variation of the AOM method that uses higher temperatures. The AOCS officially adopted the OSI method under reference Cd 12b-92 [77], with 110 °C as the standard value, although temperatures up to 140 °C are also used. This method involves bubbling purified air through the sample of fat or oil in a glass tube placed in a thermostatic aluminum heating block (Fig. 18.18a). As oxidation proceeds, the air leaving the sample passes into a container with deionized water, whose conductivity is monitored with a special electrode. The induction period or OSI value, in hours, is calculated by the equipment software as the point where a significant change in the increase in conductivity occurs (Fig. 18.18b), corresponding to the maximum of the second derivative of this with respect to time. de Man and colleagues [78] reported that the OSI value reached was mainly due to the presence of formic organic acid (more than 50%), followed by the presence of acetic, propionic, butyric, valeric, and caproic acids, as lipid oxidation products, for different types of lipids.

At present, a quick and convenient small-scale oxidation test endorsed by the AOCS (Cd-12c-16 [79] and the American Society for Testing and Materials (D 8206 ASTM International) is available. This method requires less time and handling than traditional oxidative stability techniques, making it ideal for solid, doughy, and liquid samples. Furthermore, this method boasts excellent reproducibility. Frolova and colleagues [80] and Li and colleagues [81] have both investigated the oxidative stability of oleogels using rapid testing methods. Frolova's research group conducted a study examining beeswax oleogels in sunflower oil (SO) at concentrations of 3% and 6%. The processed oleogels, as well as pure SO, were subjected to a 30-min

heating period at 90 °C. To evaluate the impact of the oleogel technology on oxidative stability, an untreated SO sample was included as a reference. Subsequently, all the samples were stored at 35 °C, and their peroxide value (PV) was assessed over a duration ranging from 0 to 144 h. The findings indicated that the oleogel production method had minimal influence on the oxidative stability of sunflower oil. However, the incorporation of beeswax as a structuring agent resulted in an elevation of the peroxide value during storage, indicating a pro-oxidant effect of beeswax dependent on its concentration in the oleogel. Therefore, after 144 h of storage, the PV (measured in mEq/kg) for the samples were approximately 2.5, 3.2, 12.8, and 14.5, respectively, corresponding to SO, SOox, oleogel 3%, and oleogel 6%.

In the international market, there are different brands of automated equipment for the determination of oxidative stability during storage.

DSC is another approach to evaluate oxidative stability as a function of temperature. In Sect. 18.3, general guidelines for this technique are provided with two differences to note. First, the calorimeter should have an alternate line to supply air (or pure oxygen if the oxidation study requires it, or nitrogen for non-oxidation control tests) to the internal cell. Second, the sample must be exposed to the flow of air or oxygen (i.e., the crucible should not be sealed). The measurement can be carried out at a constant temperature, or the sample can be subjected to a temperature sweep. The equipment software should be programmed with the desired conditions for the oxidation study. Typically, oxidative stability is evaluated at a constant temperature. In this case, the baseline response in the thermogram undergoes a significant change in its slope at the onset of oxidation, which corresponds to the oxidation induction time for the sample analyzed. In this case, the heat flux, expressed as the horizontal baseline in the thermogram, undergoes a significant change when oxidation starts, manifesting this as a deviation. In general, the crossing point of the tangents before and after the change in heat flux indicates the oxidation induction time of the analyzed sample (Fig. 18.19).

In 2002, Tan and colleagues [82] conducted a comparative investigation on the oxidative stability of various commercial vegetable oils, evaluated by both the Rancimat method and DSC at a constant temperature of 110 °C. The results of the study revealed that the DSC method produced a faster oxidative induction time compared to the Rancimat method. Depending on the type of edible oil tested, the oxidation induction time values obtained via DSC were 7–260% lower than those obtained by the Rancimat method. Given its shorter testing time, the DSC method could potentially be applied to oleogel systems.

Penalties Points

The oxidative stability technique evaluated by chemical methods involves the use of solvents and reagents for titration, which can result in the imposition of penalty points (PPs). The PPs associated with reagents used range from 2 to 6. The maintenance of the DSC necessitates the continuous flow of nitrogen, but its use does not generate PPs. The electricity consumption of a DSC, OSI, or Rancimat equipment, which exceeds 1.5 kWh in each case, contributes an extra 2 PPs. The environmental

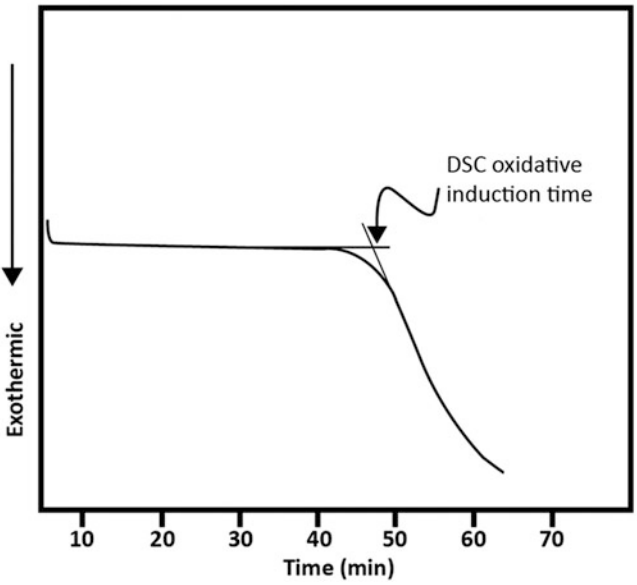

Fig. 18.19 Typical differential scanning calorimetry oxidation curve at constant temperature in an edible vegetable oil

impact of these PPs must be considered while assessing the sustainability of the oxidation technique.

Relevant Information Regarding the Technique

Spatial length scale	Cost ($, $$, $ $$)	Application	Penalty points
Atomic scale	$–$$	Quantification of oxidation products	6 when using chemical methods 8 non-automatic AOM 2 OSI-Rancimat

18.4 Thermal Characterization

18.4.1 Differential Scanning Calorimetry Technique

A differential scanning calorimeter detects endothermic and exothermic transitions due to the heat that is either provided or removed from the sample. The word "differential" is used to indicate that a sample and a reference are used and that the difference between these two is the signal reported. Although this technique does not

provide direct information about its chemical composition under given experimental conditions, it does provide useful information on the nature of the thermodynamic changes associated with the transformation of oils and fats from one physical state to another. These thermodynamic characteristics are sensitive to their general chemical composition and, therefore, can be used in qualitative and quantitative ways in their identification [83].

The complexity of the thermal profiles of fats and oils is due to the great variety of TAGs as their main constituents [84]. This is why both fats and oils do not have specific melting and crystallization temperatures, but show melting and crystallization profiles [83].

DSC devices are built according to one of two basic measuring principles: the heat-flux (HF) principle and the power-compensated DSC principle. The HF DSC allows heat to flow separately into the sample and the reference. This flow is measured while the sample temperature changes at a constant rate. For this type of DSC analysis, a crucible (also called pan) for the sample and a crucible for the reference are placed on the same platform. Integrated temperature sensors on the platform are used to measure the temperature of the crucibles. The platform is located inside one temperature-controlled furnace. Inert gas is passed through the cell at a constant flow rate.

There exist different designs of HF DSC. The one mentioned above falls in the category of platform or disk type. Another one uses cylinders instead of a platform, and the third kind is a turret type [85]. The principle is the same [85, 86] for all of them as well as the range of temperatures that they covered (≈ -50 to ≈ 500 °C).

A micro differential DSC is a modified HF DSC that has high sensitivity with a narrower temperature range (-20 to ≈ 120 °C). This type of device is ideal to study crystallization because the cooling and heating rates can be lower than 0.001 °C/min which is suitable for determining phase transitions like intermediate phases between solid and liquid, only detectable when the heating/cooling rate is very slow. When the HF DSC is used under modulation (MD) or under pressure (P), the measurement becomes very precise. Both MD and P allow the separation of endo- or exo-peaks that might overlap in the DSC scans. In MD mode, the typically linear heating ramp is overlaid with the sinusoidal function defined by a frequency and amplitude to produce a sine wave shape temperature versus time function.

In a power-compensated (PC) DSC, the temperatures of the sample crucible and the reference crucible are kept the same while both temperatures are increased or decreased linearly. This device measures the power needed to maintain the sample crucible temperature equal to the reference crucible temperature. To achieve this, the design of the DSC calls for two independent heating units or two furnaces.

The latest power compensating DSC is called the hyper PC-DSC. This is a fast scan DSC that can perform valid heat flow measurements with fast linear controlled rates (up to 500 K/min) especially by cooling, where the rates are higher than with the classical PC DSC. Standard DSC operates under 10 K/min. The benefits of such devices are increased sensitivity at higher rates providing the best results for an analysis of melting and crystallization of metals or detection of glass transition temperature (Tg) in medications.

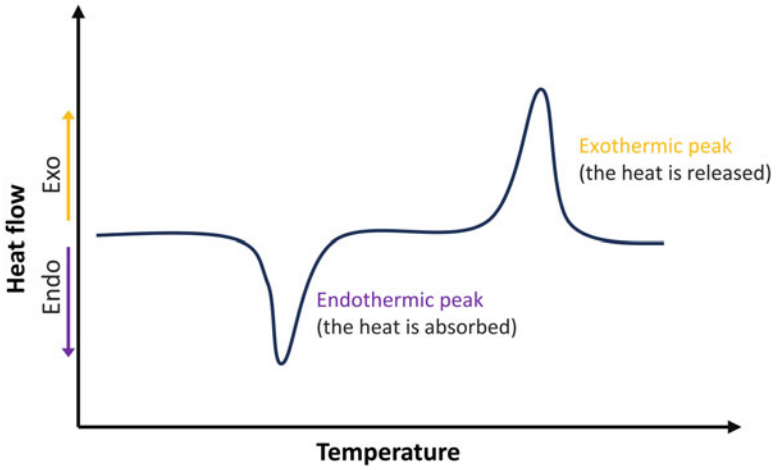

Fig. 18.20 Schematic diagram of a thermogram where heat flow was plotted as a function of the temperature (which can also be replaced by time)

Figure 18.20 shows the typical information obtained from a DSC when the temperature is either increased or decreased at a constant rate. An endothermic peak and an exothermic peak indicate the range of melting or crystallization.

Figure 18.21 illustrates the crystallization behavior of the material as measured by DSC. The data was collected by cooling the sample from 80 to 20 °C at a controlled rate, and the heat flow generated by the sample was recorded as a function of temperature. The graph clearly shows the exothermic heat flow peak associated with the crystallization process, indicating the onset and completion of the solidification process. Researchers have presented varying viewpoints regarding the characterization of the temperature at which a material undergoes crystallization. Some researchers refer to the highest point on the crystallization peak as the temperature associated with crystallization, while others consider the temperature at which the process initiates as the defining point. However, upon observing Fig. 18.20, it becomes evident that crystallization occurs within a temperature range.

The area under the peak, marked as H_c in Fig. 18.21, corresponds to the enthalpy of the phase transition (liquid to solid). If the system is under constant pressure and when the only work done in the system is due to heat, then one can equate the heat removed from the sample to the enthalpy of crystallization. Units for enthalpy are Joules (J) or J/g.

Any of the calorimeters described above can be used to study the structuring of oleogels at a constant temperature, which is an area that has been little explored until now [87]. This approach enables the determination of the induction time to structure the oleogels, as well as the enthalpy involved in the process (Fig. 18.22). For materials such as oleogels, which consist of a liquid phase and a structuring agent, the induction time is closely related to the structuring agent's concentration and its chemical structure. A change in the structuring agent concentration or a change in its chemical structure can lead to a larger or smaller induction time, indicating a larger or slower gelation process.

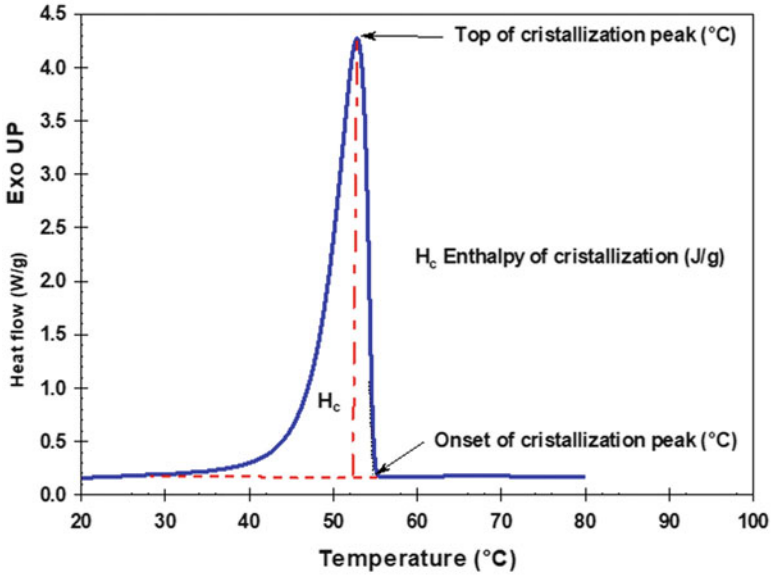

Fig. 18.21 Heat flow versus temperature showing crystallization of the material (the DSC was run by lowering the temperature from 80 to 20 °C)

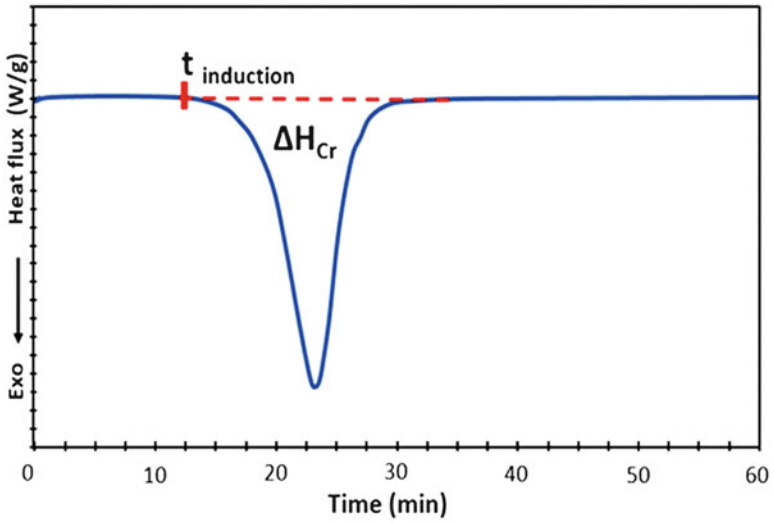

Fig. 18.22 Scheme of a DSC isothermal structuring thermogram

Penalties Points for the DSC Test

The equipment does not require any reagent or solvents to run, and the samples do not need to be prepared in any way. Hence, the PP due to the chemical used = 0. However, the equipment requires electricity to run. Runs in a DSC are never shot, requiring more than 15 min. Hence, the kWh is typically over 1.5, hence PP = 2.

Relevant Information Regarding the Technique

Spatial length scale	Operation of equipment ($, $$, $$$)	Parameters to measure	Penalty points
Millimeters micrometers	$$	Melting point Glass transition Heat capacity Enthalpy of phase transition	2

18.5 Conclusions

The objective of this chapter is to provide a thorough and all-encompassing overview of 16 techniques and methods that can be employed to investigate the structure, chemical composition, and thermal behavior of oleogels. The selection of the appropriate technique or method for investigating oleogels is dependent on the specific objectives of the study. Therefore, this chapter presents a detailed summary of each technique or method, including the length scale that it can probe and the parameters that can be evaluated. Furthermore, the Eco-Scale methodology is introduced to evaluate the environmental and health impacts of each technique by quantifying the number of reagents and solvents used and the energy consumption associated with operating the equipment using a penalty point system. It is worth mentioning that some techniques have low penalties (2 or less) as they require cheap materials such as in the oil migration studies that use filter paper or, in the consistency studies that use a manual cone penetrometer. Conversely, other techniques may have the same low penalty points but demand the use of expensive equipment, such as Raman spectroscopy. However, all techniques with more than 6 penalty points require expensive equipment and the use of reagents or solvents.

This chapter aims to raise awareness of the potential trade-offs between the cost, environmental impact, and information generated by each technique. Ultimately, minimizing the penalties points incurred during the study of oleogels can promote safe operations, reduce environmental harm, and achieve scientifically rigorous results. The information provided in this chapter can serve as a guide for researchers and professionals to select the most appropriate technique for their study of oleogels, while minimizing the impact on the environment and human health.

References

1. Gałuszka A, Migaszewski Z, Namieśnik J (2013) The 12 principles of green analytical chemistry and the SIGNIFICANCE mnemonic of green analytical practices. Trends Anal Chem 50:78–84. https://doi.org/10.1016/j.trac.2013.04.010
2. Gałuszka A, Migaszewski ZM, Konieczka P, Namieśnik J (2012) Analytical Eco-Scale for assessing the greenness of analytical procedures. Trends Anal Chem 37:61–72. https://doi.org/10.1016/j.trac.2012.03.013
3. Anastas P, Warner J (1998) Green chemistry: theory and practice. Oxford University Press, Oxford/New York
4. Anastas PT (2003) Meeting the challenges to sustainability through green chemistry. Green Chem 2:G29
5. De Man JM, Gupta S, Kloek M, Timbers GE (1984) Instrumentation for thermopenetrometry of fats. J Am Oil Chem Soc 61:1569–1570
6. Haighton AJ (1959) The measurement of the hardness of margarine and fats with cone penetrometers. J Am Oil Chem Soc 36:345–348
7. Dixon BD, Parekh JV (1979) Use of the cone penetrometer for testing the firmness of butter. J Texture Stud 10:421–434
8. de Man JM (1983) Consistency of fats: a review. J Am Oil Chem Soc 60:82–87
9. AOCS (2017) AOCS Cc 16–60: consistency, penetrometer method. In: Official methods and recommended practice of the AOCS, 7th edn. AOCS Press, Urbana
10. Gravelle AJ, Barbut S, Marangoni AG (2012) Ethylcellulose oleogels: manufacturing considerations and effects of oil oxidation. Food Res Int 48:578–583. https://doi.org/10.1016/j.foodres.2012.05.020
11. Kupiec M, Zbikowska A, Marciniak-Lukasiak K, Kowalska M (2020) Rapeseed oil in new application: assessment of structure of oleogels based on their physicochemical properties and microscopic observations. Agriculture 10:1–11. https://doi.org/10.3390/agriculture10060211
12. Chen L, Opara UL (2013) Approaches to analysis and modeling texture in fresh and processed foods – a review. J Food Eng 119:497–507
13. Gravelle AJ, Barbut S, Marangoni AG (2013) Fractionation of ethylcellulose oleogels during setting. Food Funct 4:153–161. https://doi.org/10.1039/c2fo30227f
14. Galdámez JR, Szlachetka K, Duda JL, Ziegler GR (2009) Oil migration in chocolate: a case of non-Fickian diffusion. J Food Eng 92:261–268. https://doi.org/10.1016/j.jfoodeng.2008.11.003
15. Dibildox-Alvarado E, Rodrigues JN, Gioielli LA, Toro-Vazquez JF, Marangoni AG (2004) Effects of crystalline microstructure on oil migration in a semisolid fat matrix. Cryst Growth Des 4:731–736
16. Maleky F (2012) Oil migration through fats – quantification and its relationship to structure. In: Structure-function analysis of edible fats. AOCS Press, Urbana, pp 207–230
17. Deka K, MacMillan B, Ziegler GR et al (2006) Spatial mapping of solid and liquid lipid in confectionery products using a 1D centric SPRITE MRI technique. Food Res Int 39:365–371. https://doi.org/10.1016/j.foodres.2005.08.009
18. Marty SA, Baker KB, Dibildox-Alvarado EC et al (2005) Monitoring and quantifying of oil migration in cocoa butter using a flatbed scanner and fluorescence light microscopy. Food Res Int 38:1189–1197
19. Cho K, Tarté R, Acevedo NC (2023) Development and characterization of the freeze-thaw and oxidative stability of edible rice bran wax-gelatin biphasic gels. LWT 174:114330. https://doi.org/10.1016/j.lwt.2022.114330
20. Scharf T (2007) Polarized light. In: Polarized light in liquid crystals and polymers. Wiley, Hoboken, pp 1–18
21. Rousseau D, Hill AR, Marangoni AG (1996) Restructuring butterfat through blending and chemical interesterification. 2. Microstructure and polymorphism. J Am Oil Chem Soc 73:973–981. https://doi.org/10.1007/BF02523404

22. Shi Y, Liang B, Hartel RW (2005) Crystal morphology, and textural properties of model lipid systems. J Am Oil Chem Soc 82:399–408
23. Campos R (2013) Experimental methodology. In: Structure and properties of fat crystal networks, 2nd edn. CRC Press, Taylor & Francis Group, Boca Raton
24. Mokobi F (2022) Compound light microscope- definition, principle, parts. Brightfield Microscope. https://microbenotes.com/brightfield-microscope/. Accessed 4 Apr 2023
25. Acevedo NC (2012) Characterization of the nanostructure of triacylglycerol crystal networks. In: Structure-function analysis of edible fats. AOCS Press, Urbana, pp 5–24
26. Heertje L, Leunis M, Heertje I (1997) Measurement of shape and size of fat crystals by electron microscopy. LWT Food Sci Technol 30:141–146
27. Chawla P, de Man JM (1990) Measurement of the size distribution of fat crystals using a laser particle counter. J Am Oil Chem Soc 67:329–332
28. Poot C, Dijkshoorn W, Haighton AJ, Verburg CC (1975) Laboratory separation of crystals from plastic fats using detergent solution. J Am Oil Chem Soc 52:69–72
29. Jewell GG, Meara ML (1970) A new and rapid method for the electron microscopic examination of fats. J Am Oil Chem Soc 47:535–538
30. Maleky F, Smith AK, Marangoni A (2011) Laminar shear effects on crystalline alignments and nanostructure of a triacylglycerol crystal network. Cryst Growth Des 11:2335–2345
31. Barroso NG, Okuro PK, Ribeiro APB, Cunha RL (2020) Tailoring properties of mixed-component oleogels: wax and monoglyceride interactions towards flaxseed oil structuring. Gels 6:5. https://doi.org/10.3390/gels6010005
32. Okuro PK, Tavernier I, Bin Sintang MD et al (2018) Synergistic interactions between lecithin and fruit wax in oleogel formation. Food Funct 9:1755–1767. https://doi.org/10.1039/c7fo01775h
33. Acevedo NC, Marangoni AG (2010) Characterization of the nanoscale in triacylglycerol crystal networks. Cryst Growth Des 10:3327–3333. https://doi.org/10.1021/cg100468e
34. Pink DA, Quinn B, Peyronel F, Marangoni AG (2013) Edible oil structures at low and intermediate concentrations. I. Modeling, computer simulation, and predictions for X ray scattering. J Appl Phys 114:234901. https://doi.org/10.1063/1.4847996
35. Peyronel F, Ilavsky J, Mazzanti G et al (2013) Edible oil structures at low and intermediate concentrations: II. Ultra-small angle X-ray scattering of in situ tristearin solids in triolein. J Appl Phys 114:234902. https://doi.org/10.1063/1.4847997
36. Holey SA, Sekhar KPC, Mishra SS et al (2021) Effect of oil unsaturation and wax composition on stability, properties and food applicability of oleogels. J Am Oil Chem Soc 98:1189–1203. https://doi.org/10.1002/aocs.12536
37. Gu X, Du L, Meng Z (2023) Comparative study of natural wax-based W/O emulsion gels: microstructure and macroscopic properties. Food Res Int 165:112509. https://doi.org/10.1016/j.foodres.2023.112509
38. Zetzl AK, Gravelle AJ, Kurylowicz M et al (2014) Microstructure of ethylcellulose oleogels and its relationship to mechanical properties. Food Struct 2:27–40. https://doi.org/10.1016/j.foostr.2014.07.002
39. Faller R (2021) UCD biophysics 241: membrane biology. LibreTexts, University of California, Davis
40. Sivakanthan S, Fawzia S, Madhujith T, Karim A (2022) Synergistic effects of oleogelators in tailoring the properties of oleogels: a review. Compr Rev Food Sci Food Saf 21:3507–3539. https://doi.org/10.1111/1541-4337.12966
41. Castell-Palou A, Rosselló C, Femenia A, Simal S (2013) Simultaneous quantification of fat and water content in cheese by TD-NMR. Food Bioprocess Technol 6:2685–2694. https://doi.org/10.1007/s11947-012-0912-8
42. Todt H, Guthausen G, Burk W et al (2006) Water/moisture and fat analysis by time-domain NMR. Food Chem 96:436–440
43. Peyronel F, Co ED, Marangoni AG (2017) Physical characterization of fats and oils. In: Akoh CC (ed) Food lipids, 4th edn. CRC Press, Taylor & Francis Group, Boca Raton

44. AOCS (2009) AOCS official method AOCS Cd 16b–93: solid fat content (SFC) by low-resolution nuclear magnetic resonance, direct method. In: Official methods and recommended practice of the AOCS, 6th edn. AOCS Press, Urbana
45. AOCS (2009) AOCS official method AOCS Cd 16–81: solid fat content (SFC) by low-resolution nuclear magnetic resonance, indirect method. In: Official methods and recommended practice of the AOCS, 6th edn. AOCS Press, Urbana
46. Pang M, Wang X, Cao L et al (2020) Structure and thermal properties of β-sitosterol-beeswax-sunflower oleogels. Int J Food Sci Technol 55:1900–1908. https://doi.org/10.1111/ijfs.14370
47. McNair HM, Miller JM, Snow NH (2019) Basic gas chromatography, 3rd edn. Wiley, Hoboken. E-Book 978-1-119-45078-8
48. Kaur G, Sharma S (2018) Gas chromatography-a brief review. Int J Inf Comput Sci 5:125–131
49. AOCS (2020) AOCS Ce 2–66: preparation of methyl esters of fatty acids. In: Official methods and recommended practice of the AOCS, 7th edn. AOCS Press, Urbana
50. Flores Ruedas RJ, Dibildox-Alvarado E, Pérez Martínez JD, Murillo Hernández NI (2020) Enzymatically interesterified hybrid palm stearin as an alternative to conventional palm stearin. CYTA J Food 18:1–10. https://doi.org/10.1080/19476337.2019.1699168
51. AOCS (2020) AOCS Ce 1h–05: cis-,trans, saturated, monounsaturated and polyunsaturated fatty acids in vegetable or non-ruminant animal oils and fats by capillary GLC. In: Official methods and recommended practice of the AOCS, 7th edn. AOCS Press, Urbana
52. AOCS (2021) AOCS Ce 1i–07: saturated, cis-monounsaturated, and cis-polyunsaturated fatty acids in marine and other oils containing long chain polyunsaturated fatty acids (PUFAs) by capillary GLC. In: Official methods and recommended practice of the AOCS, 7th edn. AOCS Press, Urbana
53. Delmonte P, Milani A, Kramer JKG (2021) Tutorial for the characterization of fatty acid methyl esters by gas chromatography with highly polar capillary columns. J AOAC Int 104:288–299
54. Golay PA, Moulin J, Alewijn M et al (2016) Determination of labeled fatty acids content in milk products, infant formula, and adult/pediatric nutritional formula by capillary gas chromatography: collaborative study, final action 2012.13. J AOAC Int 99:210–222. https://doi.org/10.5740/jaoacint.15-0140
55. Rumayor-Escobar A, de la Peña MM, de la Rosa-Millán J et al (2023) Effect of high intensity ultrasound on soybean and avocado oleogels' structure and stability. Food Struct 36:100315. https://doi.org/10.1016/j.foostr.2023.100315
56. Van Bockstaele F, Romanus M, Penagos IA, Dewettinck K (2022) Functionality of natural waxes in hybrid fat crystal networks. In: Development of trans-free lipid systems and their use in food products. Royal Society of Chemistry, Cryodon
57. AOCS (2009) AOCS Ce 5–86: triglycerides by gas chromatography. In: Official methods and recommended practice of the AOCS, 6th edn. AOCS Press, Urbana
58. Cordova-Barragan M, Marangoni AG, Peyronel F, Dibildox-Alvarado E (2021) Crystallization enhancement by a high behenic acid stabilizer in a palm oil-based model fat blend and its corresponding fat-reduced water-in-oil emulsion. J Am Oil Chem Soc 98:413–424. https://doi.org/10.1002/aocs.12461
59. Doan CD, To CM, De Vrieze M et al (2017) Chemical profiling of the major components in natural waxes to elucidate their role in liquid oil structuring. Food Chem 214:717–725. https://doi.org/10.1016/j.foodchem.2016.07.123
60. Castilho PC, Costa MDC, Rodrigues A et al (2004) Characterization of triacylglycerols in madeira laurel oil by HPLC-atmospheric pressure chemical ionization-MS. J Am Oil Chem Soc 81:913–919. https://doi.org/10.1007/s11746-004-1001-9
61. Jham GN, Muller HV, Cecon P (2008) Triacylglycerol molecular species variation in stored coffee beans determined by reverse-high-performance liquid chromatography/refractive index detector. J Stored Prod Res 44:82–89. https://doi.org/10.1016/j.jspr.2007.05.003
62. Amaral JS, Cunha SC, Alves MR et al (2004) Triacylglycerol composition of walnut (Juglans regia L.) cultivars: characterization by HPLC-ELSD and chemometrics. J Agric Food Chem 52:7964–7969. https://doi.org/10.1021/jf048918n

63. van der Klift EJC, Vivó-Truyols G, Claassen FW et al (2008) Comprehensive two-dimensional liquid chromatography with ultraviolet, evaporative light scattering and mass spectrometric detection of triacylglycerols in corn oil. J Chromatogr A 1178:43–55. https://doi.org/10.1016/j.chroma.2007.11.039
64. Foubert I, Dewettinck K, Van de Walle D et al (2007) Physical properties: structural and physical characteristics. In: The lipid handbook, 3rd edn. CRC Press, Taylor & Francis Group, Boca Raton, pp 535–590
65. Fauconnot L, Hau J, Aeschlimann JM et al (2004) Quantitative analysis of triacylglycerol regioisomers in fats and oils using reversed-phase high-performance liquid chromatography and atmospheric pressure chemical ionization mass spectrometry. Rapid Commun Mass Spectrom 18:218–224. https://doi.org/10.1002/rcm.1317
66. Byrdwell WC, Neff WE (1999) Non-volatile products of triolein produced at frying temperatures characterized using liquid chromatography with online mass spectrometric detection. J Chromatogr A 852(2):417–432
67. Mottram HR, Woodbury SE, Evershed RP (1997) Identification of triacylglycerol positional isomers present in vegetable oils by high performance liquid chromatography/atmospheric pressure chemical ionization mass spectrometry. Rapid Commun Mass Spectrom 11:1240–1252. https://doi.org/10.1002/(SICI)1097-0231(199708)11:12<1240::AID-RCM990>3.0.CO;2-5
68. Ross KL, Hansen SL, Tu T (2011) Reversed-phase analysis of triacylglycerols by ultra performance liquid chromatography-evaporative light scattering detection (UPLC-ELSD). Lipid Technol 23:14–16. https://doi.org/10.1002/lite.201100083
69. Fu H, Lo YM, Yan M et al (2020) Characterization of thermo-oxidative behavior of ethylcellulose oleogels. Food Chem 305:125470. https://doi.org/10.1016/j.foodchem.2019.125470
70. Kamal-Eldin A, Pokorný J (2005) Lipid oxidation products and methods used for their analysis. In: Analysis of lipid oxidation, 1st edn. AOCS Press, Urbana
71. Boatright W (2020) Commercial assay kit using novel compound semiconductor materials for measuring peroxide value in edible fats & oils. National Institute of Food and Agriculture. https://www.sbir.gov/node/1906399
72. Giacomozzi AS, Carrín ME, Palla CA (2021) Storage stability of oleogels made from monoglycerides and high oleic sunflower oil. Food Biophys 16:306–316. https://doi.org/10.1007/s11483-020-09661-9/Published
73. Park C, Maleky F (2020) A critical review of the last 10 years of oleogels in food. Front Sustain Food Syst 4:139. https://doi.org/10.3389/fsufs.2020.00139
74. Verleyen T, Van Dyck S, Adams CA (2005) Accelerated stability test. In: Analysis of lipid oxidation, 1st edn. AOCS Press, Urbana
75. O'Keefe SF, Wiley VA, Knauft DA (1993) Comparison of oxidative stability of high- and normaI-oleic peanut oils. J Am Oil Chem Soc 70:489–492
76. AOCS (1993). Surplus. AOCS Cd 12–57: fat stability, active oxygen method. In: Official methods and recommended practice of the AOCS, 7th edn. AOCS Press, Urbana
77. AOCS (2022) AOCS Cd 12b–92: oil stability index. In: Official methods and recommended practice of the AOCS, 7th edn. AOCS Press, Urbana
78. de Man JM, Tie F, Deman L (1987) Formation of short chain volatile organic acids in the automated AOM method. J Am Oil Chem Soc 64:993–996
79. AOCS (2017) AOCS Cd 12c–16: accelerated oxidation test for the determination of the oxidation stability of foods, oils and fats using the oxitest oxidation test reactor. In: Official methods and recommended practice of the AOCS, 7th edn. AOCS Press, Urbana
80. Frolova YV, Sobolev RV, Sarkisyan VA, Kochetkova A (2021) Approaches to study the oxidative stability of oleogels. IOP Conf Ser Earth Environ Sci 677(3):032045
81. Li L, Wan W, Cheng W et al (2019) Oxidatively stable curcumin-loaded oleogels structured by β-sitosterol and lecithin: physical characteristics and release behaviour in vitro. Int J Food Sci Technol 54:2502–2510. https://doi.org/10.1111/ijfs.14208

82. Tan CP, Man YBC, Selamat J, Yusoff A (2002) Analytical, Nutritional and Clinical Methods Section. Comparative studies of oxidative stability of edible oils by differential scanning calorimetry and oxidative stability index methods. Food Chem 76:385–389
83. Tan CP, Che Man YB (2000) Differential scanning calorimetric analysis of edible oils: comparison of thermal properties and chemical composition. J Am Oil Chem Soc 77:143–155. https://doi.org/10.1007/s11746-000-0024-6
84. Ali AR, Dimick PS (1994) Thermal analysis of palm mid fraction, cocoa butter and milk fat blends by differential scanning calorimetry. J Am Oil Chem Soc 71:299–302
85. Kodre K, Attarde S, Yendhe P et al (2014) Differential scanning calorimetry: a review. Res Rev J Pharm Anal 3:11–22
86. Peyronel F, Campos R (2012) Methods used in the study of the physical properties of fats. In: Structure-function analysis of edible fats. AOCS Press, Urbana, pp 231–294
87. Wang X, Ma D, Liu Y et al (2022) Physical properties of oleogels fabricated by the combination of diacylglycerols and monoacylglycerols. J Am Oil Chem Soc 99:1007–1018. https://doi.org/10.1002/aocs.12622